

**Nanostructure and microstructure fabrication
From desired properties to suitable processes**

van Assenbergh, Peter; Meinders, Erwin; Geraedts, Jo; Dodou, Dimitra

DOI

[10.1002/sml.201703401](https://doi.org/10.1002/sml.201703401)

Publication date

2018

Document Version

Final published version

Published in

Small

Citation (APA)

van Assenbergh, P., Meinders, E., Geraedts, J., & Dodou, D. (2018). Nanostructure and microstructure fabrication: From desired properties to suitable processes. *Small*, 14(20), Article 1703401. <https://doi.org/10.1002/sml.201703401>

Important note

To cite this publication, please use the final published version (if applicable).
Please check the document version above.

Copyright

Other than for strictly personal use, it is not permitted to download, forward or distribute the text or part of it, without the consent of the author(s) and/or copyright holder(s), unless the work is under an open content license such as Creative Commons.

Takedown policy

Please contact us and provide details if you believe this document breaches copyrights.
We will remove access to the work immediately and investigate your claim.

Green Open Access added to TU Delft Institutional Repository

'You share, we take care!' – Taverne project

<https://www.openaccess.nl/en/you-share-we-take-care>

Otherwise as indicated in the copyright section: the publisher is the copyright holder of this work and the author uses the Dutch legislation to make this work public.

Nanostructure and Microstructure Fabrication: From Desired Properties to Suitable Processes

Peter van Assenbergh,* Erwin Meinders, Jo Geraedts, and Dimitra Dodou

When designing a new nanostructure or microstructure, one can follow a processing-based manufacturing pathway, in which the structure properties are defined based on the processing capabilities of the fabrication method at hand. Alternatively, a performance-based pathway can be followed, where the envisioned performance is first defined, and then suitable fabrication methods are sought. To support the latter pathway, fabrication methods are here reviewed based on the geometric and material complexity, resolution, total size, geometric and material diversity, and throughput they can achieve, independently from processing capabilities. Ten groups of fabrication methods are identified and compared in terms of these seven moderators. The highest resolution is obtained with electron beam lithography, with feature sizes below 5 nm. The highest geometric complexity is attained with vat photopolymerization. For high throughput, parallel methods, such as photolithography ($\approx 10^1 \text{ m}^2 \text{ h}^{-1}$), are needed. This review offers a decision-making tool for identifying which method to use for fabricating a structure with predefined properties.

down to 10 nm and with self-cleaning,^[3] adhesive,^[4–6] antireflective,^[7] and sensing^[8] properties. In the biomedical field, nanostructures and microstructures are fabricated as antibacterial and antiadhesive coatings for implantable prostheses^[9,10] and as scaffolds for enhanced tissue regeneration.^[11] Nanofabrication and microfabrication methods are also used to make nanoelectrochemical and microelectromechanical systems (NEMS and MEMS), for example, for trapping biomolecules or biostructures,^[12] for facilitating diagnostic purposes,^[13,14] and for carrying out chemical reactions in a configurable and scalable fashion.^[15,16] MEMS and NEMS can also be paper-based, making fabricated structures disposable, or fully recyclable at low cost.^[17]

1. Introduction

Nanostructures and microstructures are used in several research and application fields. Advancements in nanofabrication and microfabrication technologies over the last decades include increasingly smaller feature sizes, enhanced functionality, and improved economic viability either for large-scale production in industry or for small-scale production in laboratory research. For example, in the information-technology industry, feature sizes of integrated circuits (ICs) are continuously scaled down, consistent with Moore's law of biennial doubling of the number of transistors on a microprocessor chip.^[1,2] In polymer sciences, researchers emulate biological structures with feature sizes

The wide array of applications for nanostructures and microstructures is accompanied by a variety of fabrication methods. Lithographic methods, such as photolithography, electron beam lithography (EBL), and ion beam lithography (IBL), are the fabrication methods of choice in the field of microelectronics,^[18] likely due to the high resolutions and throughput that these methods can achieve. Additive manufacturing (AM) of microstructures and nanostructures is gaining attention for fabrication of photonic crystals,^[19] bioinspired adhesives,^[20] and optical data storage,^[21] probably because the digital nature of the AM process allows on-demand manufacturing and thus wide diversity in structural design.^[19,22] Pattern transfer methods, such as stamping and molding, are greatly used for research purposes, as they are simple and low-cost, providing a fast and effective tool toward structures with nanometer-sized or micrometer-sized features^[23] and compatible with a range of materials, including biomaterials,^[24] polymeric materials,^[25] and paper.^[26]

The diversity of nanofabrication and microfabrication methods, their rapid progress in terms of resolution and geometric complexity, and the emergence of new fabrication methods create a need for systematic comparisons between these methods, in order to depict what is currently possible in terms of manufacturability and to identify trends in the development of fabrication methods and their applications. Several classifications of nanofabrication and microfabrication methods have been presented in the literature. Gates et al.^[23] distinguished between conventional (i.e., commercialized) and unconventional (i.e., emerging) nanofabrication and microfabrication methods, and between top-down (e.g., lithographic) and bottom-up (e.g., molecular or particle interaction and assembly)

P. van Assenbergh, Dr. D. Dodou
Department of BioMechanical Engineering
Faculty of Mechanical, Maritime and Materials Engineering
Delft University of Technology
Mekelweg 2, 2628 CD, Delft, The Netherlands
E-mail: s.p.vanassenbergh@tudelft.nl

Dr. E. Meinders
AMSYSTEMS Center
De Lismortel 31, 5612 AR, Eindhoven, The Netherlands
Prof. J. Geraedts
Faculty of Industrial Design Engineering
Delft University of Technology
Landbergstraat 15, 2628 CE, Delft, The Netherlands

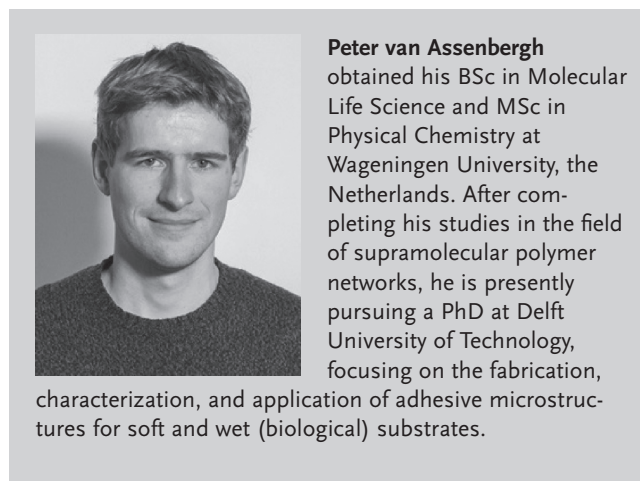
 The ORCID identification number(s) for the author(s) of this article can be found under <https://doi.org/10.1002/sml.201703401>.

DOI: 10.1002/sml.201703401

methods. These authors predicted that one of the main future trends will be the development of fabrication techniques that enable resolutions under 20 nm at low cost. Brinksmeier et al.^[27] classified nanofabrication and microfabrication methods based on two large application fields: microsystem technologies (including MEMS and micro-opto-electromechanical systems) and micro-engineering technologies (including mechanical components, molds, and microstructured surfaces). These authors observed that while each of these two fields employs a different set of preferred fabrication techniques (e.g., photolithography primarily being used in microsystem technologies and microengraving being used in microengineering technologies) (electron, ion, and laser) beam lithographic methods are used in both fields. Qin et al.^[28] divided micromanufacturing methods in traditional MEMS-based manufacturing methods and emerging non-MEMS-based manufacturing methods. A few years later, Razali and Qin^[29] presented an alternative classification based on the nature of the process used, distinguishing between additive, subtractive, deforming, joining, and hybrid processes, and argued that deforming processes, such as stamping, are highly promising for industrial applications, but that achieving high throughput in combination with precise positioning of the material in an industrial environment is a critical bottleneck. A similar classification was made earlier by Dimov et al.,^[30] based on whether a fabrication method relies on removal or addition of material, and on the number of dimensions in which processing occurs (e.g., milling being a 1D material-removal process and injection molding being a 3D material-adding process). Dimov et al.^[30] acknowledged that it is unlikely that a sole type of fabrication technology becomes dominant and highlighted the importance of integrating multiple technologies and of developing hybrid technologies. Vaezi et al.^[31] argued that MEMS technology will improve with the availability of more complex 3D microstructures and accordingly reviewed 3D microadditive manufacturing methods, classified in scalable additive manufacturing (AM) methods (with which both macroscale and microscale structures can be fabricated), 3D direct writing methods (suitable for microscale structures only), and hybrid processes (in which additive and subtractive processes are combined).

A common feature of the aforementioned classifications is that nanofabrication and microfabrication methods are categorized based on their processing characteristics. This is certainly meaningful, resonating field-dependent developments in fabrication methods. A consequence thereof might be, however, that researchers and designers could miss opportunities that are becoming available outside their fields of expertise. When designing a new nanostructure or microstructure, it may be more fruitful to choose a fabrication method based on the properties of the envisioned structure rather than deciding on the properties of the structure based on the processing capabilities of the fabrication methods at hand.

The difference between a processing-based and a performance-based decision-making can be illustrated by the three-link chain model proposed by Olson,^[32] which integrates relations between processing, structure, property, and performance, in a manufacturing roadmap. Olson distinguished between a processing-based (deductive) and a performance-based (inductive) pathway through the chain (**Figure 1**).^[32] While the deductive approach follows the path from processing toward performance, an inductive approach is also possible, according to which the



structure needed for the envisioned performance and properties is defined first, and then the most suitable processing methods are sought. Such a pathway shift is ongoing in the rapidly evolving field of AM, in which “depending on the needed structure, a suitable AM process for manufacturing can be selected that is able to create the needed structure”^[22] (see also Bourell et al.,^[33] in which such an inductive design methodology is identified as a way to assist understanding the relationships between processing, structure, properties, and performance).

To support a performance-based pathway of designing and fabricating nanostructures and microstructures, in this paper we review nanofabrication and microfabrication methods based on the geometric characteristics and the materials the structure is made of, independently from the processing characteristics of the fabrication methods (e.g., subtractive vs additive, top-down vs bottom-up) and their current application fields (e.g., nanoelectronics or microelectronics, bioengineering, etc.). Accordingly, we review nanofabrication and microfabrication methods based on the following four moderators:

- **Geometric Complexity:** Geometric complexity refers to the architectural design of a functional nanostructure or microstructure,

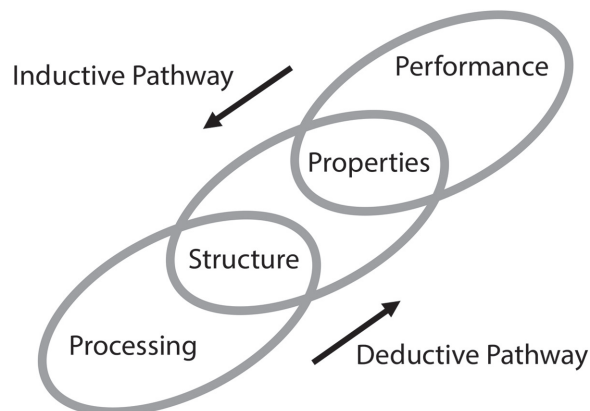


Figure 1. Three-link chain model integrating the relations between processing, structure, property, and performance of an engineered structure. Adapted with permission.^[32] Copyright 1997, The American Association for the Advancement of Science.

the complexity of which we consider increasing with the presence of geometric features such as curvatures, cavities, and overhangs. We define three levels of increasing geometric complexity, ranging from 1 to 3, which will be introduced later in this section.

- **Material Complexity:** With material complexity we refer to the number of materials that can be used in one structure, resulting in integration of materials with different values of the same material property (e.g., variable degrees of stiffness) or integration of materials serving different properties (e.g., one material for low stiffness and another material allowing for conducting regions in the structure). We define two levels of material complexity, single (one material in the structure) and multiple (two or more materials in the structure).
- **Resolution:** Resolution is defined as the smallest volume that can be added to or removed from a structure. This volume is determined by both the size of the smallest piece of matter that can be added or removed (which is sometimes referred to as the smallest feature size) and the minimal spatial separation between two added or removed pieces of matter.^[34] The minimal spatial separation is determined by the attainable placement accuracy and/or by the properties of the material that is added or removed. Here, we use a 4-point scale to quantify resolution, ranging between ≤ 10 nm, 11–100 nm, 101 nm–1 μm , and > 1 μm .
- **Total Size:** Total size refers to the maximum attainable total area of the structure. We use a 4-point scale to quantify the total size of nanostructures or microstructures, ranging between < 1 mm^2 , 1–99 mm^2 , 1–10 cm^2 , and > 10 cm^2 .

The contribution of each of these four moderators to the performance of a nanostructure or microstructure varies between applications. For example, performance of patterned adhesives is predominantly determined by their geometric complexity (e.g., mushroom-shaped pillars,^[35] hierarchical structures^[36]), but high resolution (i.e., small size of features^[37]) and the use of more than one material in the structure^[38] can also be employed for enhancing adhesion. Another example is MEMS, the performance of which is assumed to improve with miniaturization of these systems, leading to higher processing speeds, energy conservation, and cost reduction.^[39] Application of nanoscale components (as is done in NEMS) introduces even more functionalities, including space-efficient and light-weight structures or high mechanical resonance frequencies.^[39,40] However, next to resolution, material complexity (i.e., integration of different materials^[41]) and geometric complexity (e.g., stacked architectures^[41,42]) also contribute to the performance of MEMS.

Next to the four above-mentioned moderators of a single nanostructure or microstructure, an important criterion in deciding which fabrication method to use is the flexibility of methods, that is, the extent of the output, both in terms of diversity and in terms of size. Accordingly, in this review we also include the following three moderators:

- **Geometric Diversity:** With geometric diversity we refer to the variety of shapes that can be fabricated with the same instrumental setup. For example, with one 3D mold only one geometry can be made, whereas with a scanning beam lithography (SBL) setup multiple geometries can be made. We define geometric

diversity based on the number of dimensions (between zero and three) in which a structure can be independently tuned. For example, for imprinting methods, this number would be zero, whereas for a scanning-beam lithographic method, the structure is freely tunable in two dimensions (with the possibility of linearly extruding a 2D pattern in the third dimension by varying etch depth).

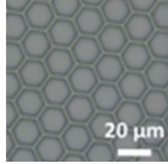
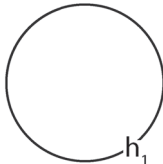
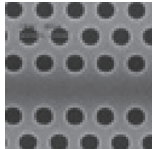
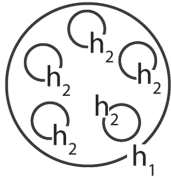
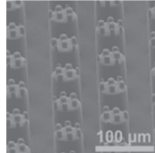
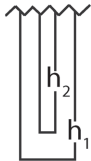
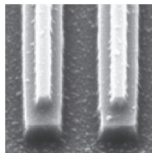
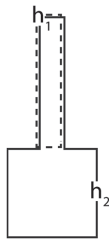
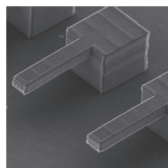
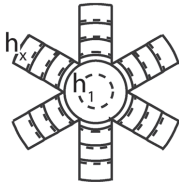
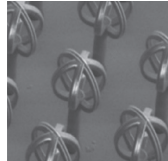
- **Material Diversity:** With material diversity we refer to the variety of material types of which a nanostructure or microstructure can be made. A fabrication method that allows for higher material diversity can be used to attain structures with a greater variety in material properties (e.g., structures with various degrees of stiffness or refractive indexes). We define two levels of material diversity, in which level 1 implies that the fabrication methods can accommodate only one group of materials (e.g., only metallic materials, or photosensitive materials, or biomaterials), and level 2 implies compatibility with more than one group of materials.
- **Throughput:** Throughput refers to fabrication speed. Depending on the type of fabrication method, throughput is expressed in “writing length per second,”^[19,43] “area or volume per hour,”^[19] or “wafers per hour.”^[44–46] Here we use a 4-point scale to characterize throughput, ranging between low, medium, high, and very high. A low throughput means fabrication speed in the order of a few mm^2 per hour, a very high throughput is in the order of tens of mm^2 per hour.

In recent years, the quest for functional structures inspired by nature raised great interest in the relation between function (e.g., light harvesting,^[47] impact-resistance,^[48] adhesion^[49,50]) and properties (e.g., strength, toughness, stiffness) by means of varying structural rather than material properties.^[51,52] Indeed, to meet the natural equilibrium between material formation and degradation,^[51] biological materials are limited in both number and performance (e.g., natural materials are typically soft or brittle^[52,53]), and exceptional properties originate from geometric complexity, rather than from the used materials. An example thereof is the impact-resistant club of smashing stomatopods, which is used to hammer the shells of prey. The high strength of the club originates from a specific architecture, namely a helicoidal arrangement of mineralized chitin fibres, resulting in a so-called Bouligand geometry.^[54]

Following this rationale, we chose to classify the fabrication methods based on the geometric complexity that can be attained with them. We operationalize geometric complexity based on the number of isolines, also referred to as contour lines,^[55] required to describe the topology of the structure (or of one module of the structure, in the case of a periodic structure, that is, a structure consisting of repetitive modules) and define accordingly three levels of geometric complexity (Table 1). We borrowed the concept of isolines from physical geography (among other fields), where isolines are commonly used as an effective 2D representation of 3D landscapes and surfaces. We defined the three levels of geometric complexity.

- **Level 1:** 2D structures, extruded in the third dimension with a fixed extrusion height or depth. When a 3D structure is an extrusion of a planar pattern with a fixed extrusion height or depth, one isoline, with a nonzero height or depth, is required to describe the structure.

Table 1. Levels of geometric complexity.

Geometric complexity level	Contour map	Examples and applications
<p>Level 1. 2D structures, extruded in the third dimension with a fixed extrusion height or depth. The structure is an extrusion of a planar structure with a fixed height or depth. One isoline, with a nonzero height (or depth) h_1, is required to describe the structure.</p>		 <p>Patterned adhesive consisting of hexagonal pillar arrays, fabricated using molds made with photolithography. Adapted with permission.^[6] Copyright 2015, John Wiley and Sons.</p>
		 <p>2D photonic crystals, deposited and self-assembled on a silicon substrate. Adapted with permission.^[57] Copyright 2017, The Japan Society of Applied Physics.</p>
<p>Level 2. 3D structures with areas of various heights and no overhanging parts or cavities. Two or more isolines are required to describe the structure, and for all pairs of isolines it holds that if $h_2 > h_1$, then $l_2 \leq l_1$, where l is the isoline length and h is the isoline height.</p>		 <p>Hierarchical adhesive, fabricated with a two-step molding process. Adapted with permission.^[58] Copyright 2009, John Wiley and Sons.</p>
		 <p>Two-level lines on a substrate, to be cut into T-shaped particles. Made with imprinting lithography. Adapted with permission.^[56] Copyright 2017, Springer Nature.</p>
<p>Level 3. 3D structures with overhanging parts and/or cavities. The contour map either contains at least one pair of isolines for which it holds that if $h_2 > h_1$, then $l_2 > l_1$ (top picture; the isoline with height h_1 is located partially under the isoline with height h_2), or contains overlapping (i.e., crossing) isolines (bottom picture). The dashed lines are located below the solid lines and are slightly shifted (laterally at the top picture and radially at the bottom picture) for the sake of visibility.</p>		 <p>Microcantilevers to be used for quantifiably evaluating the mechanical properties of the material the structure is made of. Adapted with permission.^[59] Copyright 2012, AIP Publishing LLC.</p>
		 <p>An air-trapping surface to be used underwater. Fabricated with stereolithography. Adapted with permission.^[60] Copyright 2015, American Chemical Society.</p>

- *Level 2:* 3D structures with areas of various heights and no overhanging parts or cavities. Two or more isolines are required to describe such structures, and for all pairs of isolines it holds that if $h_2 > h_1$, then $l_2 \leq l_1$, where h is the height

of the isoline and l is the length of the isoline. The larger the variability in heights (cf. structures with curved surfaces), the larger the number of isolines required to describe the structure.

- *Level 3:* 3D structures with overhanging parts and/or cavities. The contour map either contains crossing isolines or there is at least one pair of isolines for which it holds that if $h_2 > h_1$, then $l_2 > l_1$.

These levels of geometric complexity are comparable to three shape categories for particles in a dispersion, as presented in Reuter et al.,^[56] who distinguished between “quasi 2D” (shaped in plane), “hemi 3D” (shaped in half space), and “fully 3D” (shaped in the entire space).

In the remainder of the paper, nanofabrication and microfabrication methods are presented in order of ascending geometric complexity; for each fabrication method, we briefly describe the working principle and assess the method in terms of the aforementioned moderators. In the discussion section, a decision tool is presented, in which all seven moderators are taken into consideration simultaneously.

2. Fabrication Methods for 2D Structures Extruded in the Third Dimension with a Fixed Extrusion Height or Depth (Geometric Complexity Level 1)

Nanostructures and microstructures of which the third dimension is an extrusion of a 2D pattern can be manufactured by means of scanning probe lithography (SPL), photolithography, scanning (ion or electron) beam lithography, colloidal lithography, and block-copolymer lithography.

2.1. Scanning Probe Lithography

In SPL, a scanning probe tip is used to pattern substrates in either an additive (so-called additive SPL) or a subtractive (called subtractive SPL) fashion by transferring molecules toward or from a substrate mechanically, diffusively, electrically, or thermally.^[61] SPL can be realized with a standard atomic force microscope (AFM), making SPL an accessible, versatile, and appealing method for nanoscale engineering.^[61,62] The main advantage of SPL is that, with piezoelectric positioning of the scanning probe tip, resolutions of 10 nm can be achieved in a direct-writing step.^[63] Structures are freely written in or on a substrate, and are thus tunable in two dimensions. Due to their serial character, a limitation of SPL methods is that throughput is typically low: writing speeds are in the order of micrometers per second, and higher writing speeds typically go at the expense of resolution. One approach to increase the throughput with SPL is to use multiple tips simultaneously.

Processing conditions are generally mild in terms of temperature and stress on the sample, and a wide range of materials and substrates can be used, including biomaterials and soft matter.^[61] Furthermore, some SPL techniques allow for patterning with different materials either simultaneously^[64] or consecutively.^[65,66]

For a review on SPL techniques and their applications, see Garcia et al.^[61]

2.1.1. Additive Scanning Probe Lithography Methods

Additive SPL methods are based on deposition of material on a substrate to form a pattern. Here, we discuss dip pen

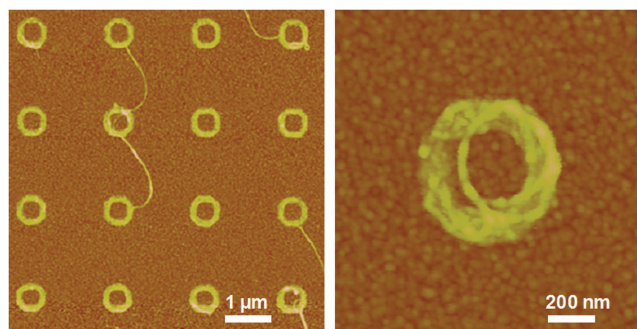


Figure 2. Left: Single-walled carbon nanotubes on a gold substrate, arranged in circles. Right: Close-up of one nanotube. Self-assembly of the nanotubes was directed on circular 16-mercaptohexadecanoic acid arrays created on a gold substrate by means of dip pen nanolithography (DPN). Reproduced with permission.^[68] Copyright 2006, National Academy of Sciences.

nanolithography (DPN) and bias-induced SPL. In DPN, an AFM tip is used to transfer molecules or a liquid ink to a substrate by molecular diffusion or fluid flow, respectively.^[63,67] DPN is a fitting tool for patterning biomaterials, because of the absence of harsh post-treatments such as ultraviolet, ion-beam, or electron-beam irradiation, and due to its high compatibility with soft matter.^[67] The thickness of the deposited layer depends on the used material that is deposited, and is fixed throughout the whole structure. DPN has been used to pattern self-assembled monolayers of molecules for trapping oligonucleotides, viruses, or proteins.^[23] Another example of patterning self-assembled monolayers with DPN was presented by Wang et al.,^[68] who used DPN to pattern a gold substrate with circular 16-mercaptohexadecanoic acid arrays, on which self-assembly of single-walled nanotubes (SWNTs) was then directed (**Figure 2**).

To increase throughput, Chen et al.^[69] used 55 000 tips simultaneously to write a pattern of initiator molecule on a gold substrate, on which a resist layer was grown. In a subsequent etching step, the written pattern was transferred into the underlying gold substrate.

Bias-induced SPL is another additive SPL method, in which a voltage is applied over the AFM probe and the substrate, to induce local deposition or transformation.^[61] For example, Ferris et al.^[70] coated a substrate with a polymer brush and then used bias-induced SPL to electrochemically pattern the surface of the polymer brush. Such electrochemical patterns can act as templates for self-assembly or for local deposition of inorganic molecules.

2.1.2. Subtractive Scanning Probe Lithography Methods

Subtractive SPL methods include thermal SPL and some forms of bias-induced SPL. Thermal SPL is an SPL method in which the substrate is altered by means of evaporation induced via a heated tip. By varying the tip temperature, the writing depth can be controlled with an accuracy down to 10 nm.^[71,72] Bias-induced SPL is also used in a subtractive fashion, inducing electrochemical processes to remove matter. For example, by locally inducing oxidation, nanopatterns can be written.^[61,73] Because of the time needed for the tip–substrate interaction to take place, most types of electrical SPL (whether additive or subtractive) come with low writing speeds.^[19] In subtractive SPL, substrate–tip interactions can also be of mechanical nature, such as scratching.^[74]

With SPL, typically single-layer structures are fabricated. A recent paper on SPL has shown that it is possible to use SPL to print structures in a layer-by-layer fashion, resulting in structures with various heights throughout the structure.^[75] If SPL turns out to be an established method for such structures, SPL will be upgraded to a complexity level-2 method.

2.2. Photolithography

In photolithography, a photoresist layer is applied on a substrate. Then, the photoresist layer is exposed to light through a photomask, that is, a planar array with transparent and opaque regions that form a pattern. Upon light exposure, the chemical stability of the photoresist changes, and depending on the type of the photoresist, either the exposed (in the case of a so-called positive resist) or unexposed (negative resist) areas of the photoresist become soluble. In a subsequent etching step, the chemically altered areas of the photoresist are removed, resulting in a patterned photoresist layer. Next, the photoresist is hardened to obtain the final structure.^[23]

Besides photosensitivity, photoresist materials need to have specific requirements, such as etch resistance, adhesion to the underlying substrate, or ability to form defect-free thin films.^[76] Commonly used photoresists are SU-8, polyimide, and Parylene C.^[77] When photolithography is used for the fabrication of ICs, the patterned photoresist acts as template for patterning the underlying semiconducting silicon layer in a subsequent etching step, and the resist is removed after pattern transfer.^[76] Due to the parallel nature of photolithography, complete layers are patterned in a single-step exposure or etch. Therefore, multilayer or multimaterial structures can only be made with post-processing or repeating exposing and etching cycles.

The attainable geometric diversity with photolithography is low, since a 2D pattern (the mask) acts as template to fabricate an extruded structure. The only freely tunable dimension is the height or depth of the structure, which can be controlled by choosing the resist layer thickness. Photolithography has a parallel nature, meaning that 2D arrays can be fabricated in a single exposure step, and feature sizes in the μm -range were obtained already in the 1970s.^[78] The method was therefore rapidly adopted by the industry, particularly for the fabrication of ICs and printed circuit boards.

In both industrial and laboratory settings, the basic principle of photolithography is the same, but moderators such as throughput and resolution can be very different. Industrial photolithographic instruments have been drastically evolved in terms of throughput and resolution by means of automatization and optimization of the instrumentation. The required instrumentation is costly,^[79] but with such optimized setups, structures can be fabricated at throughputs of more than 100 wafers per hour (equivalent to over $28 \text{ m}^2 \text{ h}^{-1}$),^[80] making the costs per patterned area relatively low.

On laboratory level, photolithography is used for fabrication of, among other applications, bioinspired adhesive microstructures^[4,6] and microfluidic chips,^[81,82] because great geometric diversity (with the use of a different photomask for each structure) and reasonable resolutions (in the order of micrometers) are possible with lab-scale photolithographic setups. Expensive

optics and automatization machinery are not required for such research purposes, and therefore the costs of a photolithographic lab instrument can be two orders of magnitude lower as compared to industrial setups.

Depending on the distance between the photomask and the substrate, three types of photolithography can be distinguished: projection photolithography, proximity photolithography, and contact photolithography. Another parallel lithographic method is plasmonic lithography. Finally, lithography with light can be also used without masks. Such maskless optical lithographic methods will be discussed in Section 2.3.

2.2.1. Projection Photolithography

Projection photolithography is sometimes referred to as far-field (optical) lithography,^[83] because a distance between the mask and the substrate has to be maintained. An optical lens (or a series of mirrors and lenses) is located between the mask and the substrate, focusing the light after it passes the mask and allowing pattern-size reduction of 2–10 times with respect to the mask.^[83] The high resolutions that can be attained (down to 37 nm)^[83] in combination with the high throughput make projection photolithography the most common method for fabricating ICs.^[84]

The main challenge of projection photolithography is that at high resolutions, the mask acts like a diffraction grating.^[85] To cancel out diffraction effects, expensive phase-shifting optics and high-sensitive photoresists are required.^[86] With the introduction of deep UV lasers, the wavelength was reduced from 365 to 248 nm in 1995 and to 193 nm in 2000,^[87] minimizing these diffraction effects. Resolutions down to 37 nm with a 193 nm wavelength excimer laser have been demonstrated.^[83] With an expected wavelength of 13.5 nm, the use of extreme ultraviolet lithography (EUV) has resulted in resolutions below 10 nm.^[88] With the use of double-patterning (or multiple-patterning), in which a pattern is split in two (or more) masks that are subsequently projected into the resist layer, patterns with a higher density and resolution than the used masks can be obtained.^[87]

Besides photons, also ions can be used with masks to transfer patterns into resist layers, as is done in ion projection lithography.^[89,90] With ion projection lithography, thanks to lower diffraction effects than with photon projection lithography, a high accuracy can be obtained, although obtainable resolutions are lower.^[90]

2.2.2. Proximity Photolithography

In proximity photolithography, the distance between photomask and photoresist is much smaller than in projection photolithography, and no optics are used to downsize the projection, significantly suppressing the costs as compared to projection photolithography.^[83] The attainable resolution with proximity (photo) lithography can improve by decreasing the laser wavelength λ and the proximity length x between the mask and the substrate according to $\sqrt{\lambda \cdot x}$.^[91] To obtain resolutions below 30 nm, the proximity length has to be at the sub-micrometer level, which is challenging.^[92] At the beginning of the 21st century, methods

were developed to correct for or even exploit Fresnel diffraction at the photomask, allowing larger mask–substrate distances.^[91]

Due to the absence of expensive optics, proximity photolithography is a cost-effective technique, considering the resolutions (2–3 μm) and throughput that can be obtained with it.^[83] Recently, EUV proximity lithography has been used for the fast fabrication of arrays of infrared antennas with feature sizes in the μm -range.^[92]

2.2.3. Contact Photolithography

In contact photolithography, the proximity length x is brought to zero, that is, the mask and the resist layer are in contact.^[93] Linewidths of around 16 nm have been fabricated using gratings in contact with the resist.^[94] The downside of this method is that the contact can cause defects on the mask or resist layer, which is the main reason why contact photolithography is not the photolithographic method of choice for industry.^[95]

2.2.4. Plasmonic Lithography

In plasmonic lithography, a thin metal plate is mounted on a prism of (typically) glass prism. When a light beam hits the metal plate through the prism at a certain incident angle, the normal component of the light wave vector couples with the wave vector of surface plasmon polaritons (SPPs) in the metal. Because of the permittivity difference between the metal and the supporting glass, this photon–SPP coupling induces SPPs propagating along the metal surface with frequencies much higher than the photons used to induce them. In plasmonic lithography, this phenomenon is used to pattern a resist layer with SPPs.

A challenge with plasmonic lithography is that SPPs decay faster than photons (in the order of 5–20 nm), only allowing for proximity lengths that are much shorter than those achieved with proximity photolithography.^[96] Feature sizes down to 22 nm have been demonstrated, by projecting a ring-shaped interference pattern of plasmonic oscillations on a resist layer.^[97] By giving the metal surface a typical curvature, high intensities of SPPs can be generated very locally, resulting in even smaller writing beams. A recent example of this is the incorporation of bowtie-shaped apertures in a metal layer. SPPs were collected at the narrowest part of the bowtie, resulting in a writing spot with diameters down to 16 nm.^[94]

2.3. Scanning Beam Lithography

Direct-writing lithographic methods are referred to as SBL. In SBL, a pattern is written on a resist layer by one or more scanning beams of photons, electrons, or ions. Note that the “resist” layer does not necessarily act as a etch-resistant layer, but rather as the layer that is manipulated. SBL methods are often used for the production of lithographic masks.^[83]

Similar to masked lithographic methods, with scanning-beam fabrication methods a pattern is freely written on or in a planar substrate. The extrusion depth of the 2D pattern is determined by the resist thickness or the beam intensity. The attainable

resolution of SBL methods improves with lower beam intensities, which reduce the beam spot size. As a consequence, the search for resists with higher sensitivities (i.e., reacting at exposure to low-intensity beams) is a critical element in SBL.^[98] Due to the serial character of SBL, manufacturing speed is slow: it can take 24 h to pattern a 1 cm^2 array with 20 nm features.^[23] SBL-fabricated structures are geometrically complex and diverse, and therefore, SBL-fabricated structures are commonly used as templates (molds or masks). Materials for resists that are compatible with SBL are limited, because they need to be photon-, electron-, or ion-sensitive. Here, we discuss optical beam lithography (OBL), interference lithography, electron beam lithography, and ion beam lithography.

2.3.1. Optical Beam Lithography

In OBL, also referred to as maskless photolithography, 2D structures with a defined height or depth are written in or on a planar substrate using UV light. Photons react with the substrate atoms by means of the photoelectric effect or by initiating photopolymerization to reduce or increase the etch resistance of a resist layer. Depending on the used resist, resolutions of about 50 nm can be achieved with OBL.^[34] Similar to masked photolithography, using light with shorter wavelengths (e.g., EUV: 13.5 nm) reduces diffraction effects. With OBL, where the photoresist is cured by means of photopolymerization, the depth of polymerization can be defined by tuning the photon intensity at the focal point of the beam. Therefore, OBL is used to write nanometer-sized lines with a defined height on a substrate.^[99] Due to this tunable polymerization depth, OBL is also suitable for the fabrication of stacked 2D projected structures, resulting in level-2-complexity structures.^[34]

2.3.2. Interference Lithography

Interference lithography (also referred to as holographic lithography) is a variant of OBL, in which the interference pattern of two coherent beams is projected on a resist layer.^[100] Alternatively, beams (or one wide beam) are diffracted with gratings to generate interference patterns.^[84] When using the second order intersect of two interfering beams, the pathway between light source and substrate is elongated, resulting in further pattern size reduction (sub 10 nm linewidths with EUV lasers).^[101] Interference lithography has the limitation that the resist layer can only be patterned with periodical structures.^[84]

2.3.3. Electron Beam Lithography

In EBL, electrons are accelerated toward a resist layer on a substrate. The dominant mechanism of EBL is electron–electron collision, resulting in either crosslinking (in case of a negative resist) or scissoring (in case of a positive resist) of the polymeric resist layer.^[102] Subsequently, a developing step (e.g., etching) is required to obtain a pattern. The resist layer can be made of hydrogen silsesquioxane (HSQ), poly(methyl methacrylate) (PMMA), NaCl, SiO₂, or LiF.^[103] The use of a high-sensitive

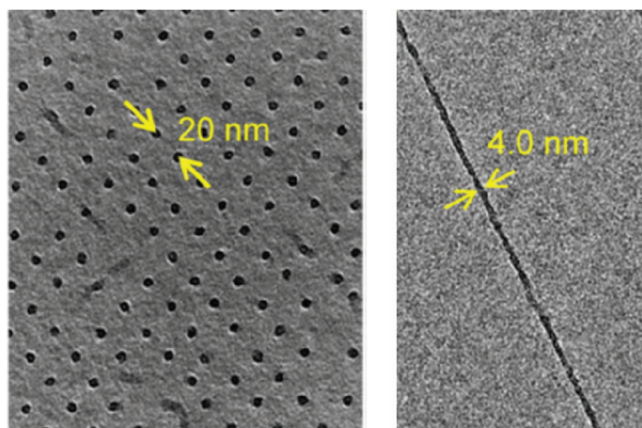


Figure 3. Left: A dot array in hydrogen silsesquioxane (HSQ), fabricated with electron beam lithography. The center-to-center distance between two dots is 10 nm, and the diameter of one dot is 5.1 nm. Right: An isolated line in HSQ, with 4 nm width. This is the smallest obtainable width at which the line did not collapse during development. Adapted with permission.^[104] Copyright 2013, American Chemical Society.

resist such as HSQ improves the resolution of EBL, but this comes with the disadvantage that HSQ has a high susceptibility for beam scattering and back-scattering at the resist;^[102] by defining and predicting the back-scattering, however, structures with sub 5 nm feature sizes have been fabricated (Figure 3).^[104] This resolution limit is not determined by the electron beam diameter, but by the mechanical strength of the resist during the subsequent developing step. In EBL, high resolution comes with a low electron dose, and therefore goes at the expense of throughput.^[104]

2.3.4. Ion Beam Lithography

IBL is a collective name for techniques in which a focused beam of ions is used to modify a surface by altering its structure or chemical properties, or by atom removal.^[105] An advantage of IBL as compared to EBL is that ions scatter less than electrons upon collision with the resist layer, minimizing collateral modifications of the resist.^[105] Moreover, ion beams have a higher impact on the substrate, meaning that a lower dose suffices to leave a pattern.^[105]

Focused ion beam lithography (FIB) is an IBL method in which heavy ions (typically Ga⁺ ions, around 30 keV) are used. The heavy ions alter the substrate upon colliding. Depending on the resist, the substrate is milled, ions are implanted, or the substrate is sputtered.^[90,105] FIB was invented in the 1970s and became commercially available 10 years later.^[90] A beam spot size of 8 nm has been reported and used to write 10 nm sized features in a 30 nm thick layer of PMMA.^[106] In Figure 4, 8 nm wide lines, written in a 50 nm thick resist layer of AlF₃/GaAs, are depicted. Such small features were obtained thanks to vaporization of the resist upon etching, which filters the edges of the ion beam and leads to a peak intensity in the center of the ion beam.^[107]

p-beam writing is another IBL method, in which protons are used to write directly and deeply in a resist layer.^[90] Protons are light and fast ions, with energies typically in the MeV range,

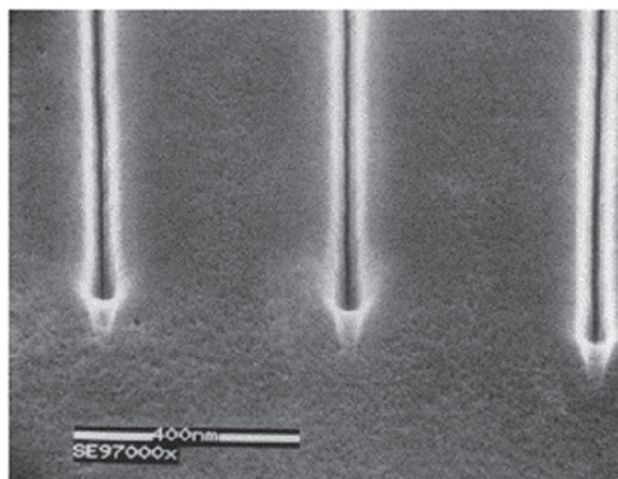


Figure 4. Lines with a width of 8 nm in an AlF₃/GaAs resist, fabricated with focused ion beam lithography. Reproduced with permission.^[107] Copyright 1999, Elsevier.

which interact with substrate ions and undergo thousands of collisions before they are adsorbed. Contrary to the heavy ions used in FIB, light-ion beams show minimal internal scattering. Moreover, light ion beams have well-defined penetration depths, which is useful for manipulating one (thick) resist layer at several depths to create multilayered structures.^[90]

2.4. Directed Self-Assembly of Planar 2D Structures

By directing the self-assembly of macromolecules on a substrate, a variety of planar patterns can be made. These patterns act as templates that are transferred into or onto underlying layers by means of etching, deposition, or stamping in parallel high-throughput processes.^[108,109] As such, 2D patterns, which are extruded in the third dimension with a fixed extrusion height or depth, can be generated.

Self-assembled templates can be fabricated by tuning the physical or chemical properties of self-assembling (macro)molecules such as block-copolymer (BCPs) or colloids upon deposition on a substrate.^[110] DNA has also been used as building block for nanoscale structures. Folding and self-organization of DNA molecules can be directed by, for example, using predefined base pair sequences obtained from enzymatic synthesis.^[111] In this section, we discuss block-copolymer lithography, colloidal lithography, and nanoporous anodic aluminum oxide (AAO).

2.4.1. Block-Copolymer Lithography

In BCP lithography, a thin film of self-assembled block-copolymers on a substrate is used as a lithographic mask after selective removal of one block by dissolving or etching. Self-assembly of BCPs can be driven by phase separation of the two (or more) blocks, induced by, for example, dissolving the polymer in a solvent, temperature modification, or acidity modification. Self-assembly of BCPs on a substrate can also be induced

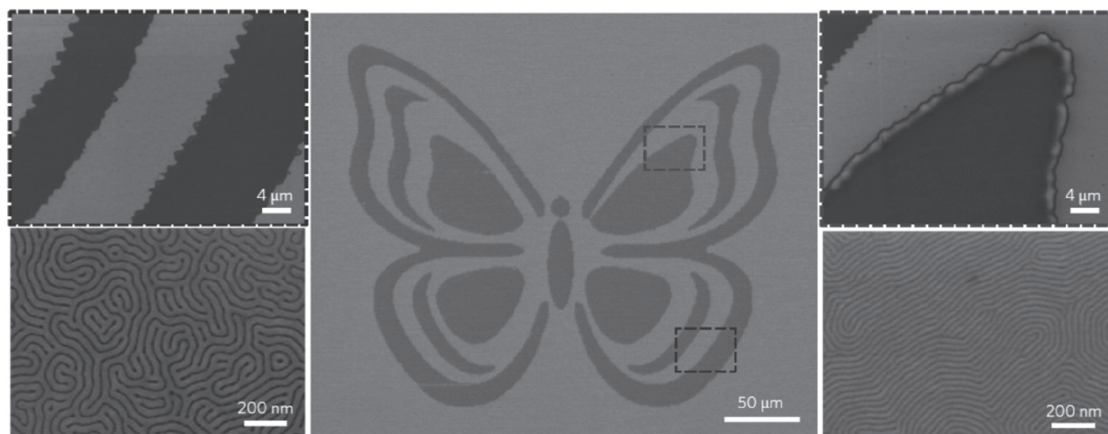


Figure 5. Electro-hydrodynamic jet printing of a butterfly from microdroplets of BCP solution. The light and dark colors originate from the use of two PS-*b*-PMMA, with different block sizes. The images left and right show magnifications of dark and light regions. The fingerprint-like patterns at the bottom two images are the result of BCP self-assembly. Reproduced with permission.^[116] Copyright 2013, Springer Nature.

by modifying the supporting substrate to create initiation point of self-assembly, for example, by applying defects using IBL^[105] or pattern high-affinity regions using SPL.^[112] By incorporating etch-resistant blocks in the BCP, the BCP pattern is transferred to an underlying functional layer through etching.^[108,113,114] Alternatively, a metallic layer can be evaporated on top of the self-assembled pattern; subsequent lift-off of the polymer layer leaves the desired pattern on the underlying substrate.^[115] Onses et al.^[116] integrated self-assembly of block-copolymers with electro-hydrodynamic jet printing (EHD; see Section 3.1.1) by printing microdroplets of BCPs dissolved in an organic solvent (Figure 5).

The resolution of BCP lithography can be tuned with the BCP block sizes and chemical properties, and is typically in the order of 10 nm.^[108] Line widths of 6 nm have been also reported.^[117] Materials used as BCP include polystyrene (PS), PMMA, poly(ethylene-alt-propylene), and poly(vinylpyridine).^[114] Because of its relatively low costs and high attainable resolutions, BCP lithography is used for the fabrication of nanopatterns for IC fabrication, photonics, and membrane fabrication.^[113,118] With photolithography being pushed to its resolution limits at the expense of high costs, BCP lithography is a very promising method for semiconductor manufacturers in their search for ever smaller feature sizes.^[108] Fundamental geometries required in IC fabrication, including lines, dots, t-junctions, bends, and jogs, can be obtained using directed self-assembly (DSA).^[119] Next to being used as templates, self-assembled layers are used as functional thin films or ordered nanoparticle arrays,^[19] photonic structures,^[120] and antireflective coatings.^[121]

BCPs can also self-assemble into 3D structures. We will discuss these structures under Section 4.

2.4.2. Colloidal Lithography

Colloidal lithography, also referred to as nanosphere lithography, is a special type of contact photolithography, in which,

instead of a patterned photoresist layer, colloids are used as a 2D template. The colloidal pattern can be transferred by means of etching (in which, similar to BCP lithography, etch-resistant colloids act as a positive resist), deposition or evaporation (with subsequent lift-off of the colloids), or imprinting.^[122,123] Colloidal lithography is a cost-effective nanofabrication method, and has been used to fabricate nanohole arrays, often used in nanophotonic devices.^[124] Lithographic masks from colloids can be further used to create triangular patterns, nanorings, and pillars.^[125] In colloidal lithography, polymeric colloids (made of, e.g., PS^[126]) and metallic colloids are most commonly used. When a colloidal crystal is used as an etch-resistant mask, the underlying layer consists of, for example, a polymeric layer,^[127] glass,^[128] or silica.^[129] Deposition with colloidal templates is typically done with metallic materials.^[130] The attainable material complexity with colloidal lithography is low, since the colloidal pattern is transferred or deposited into a single-material layer.

2.4.3. Nanoporous Anodic Aluminum Oxide

When carried out in an acid electrolyte, the anodic oxidation of aluminum results in a nanoporous layer of aluminum oxide.^[131] In a method referred to as nanoporous AAO, size and distance between pores are controlled in a two-step anodization process. Before anodization, a substrate of aluminum is electropolished to obtain a nanoscale flat substrate. Subsequently, in the first anodization step, pores are grown with various interdistances and at various angles. Upon the removal of the oxide layer, a homogeneous array of nanoscale dimples is revealed, covering the aluminum substrate. These dimples form the onset for pore growth during a second anodization step, resulting in a homogeneous pore array in an aluminum oxide layer. By varying the applied voltage during oxidation, the viscosity of the electrolyte, or the temperature, the pore size, and center-to-center distance between the pores can be varied.^[132,133] With AAO, Buijnsters et al.^[134] developed a range of structures with tunable wettability by tuning the pore array. AAO surfaces can also be used as

templates to shape polymer layers by imprinting, or for fabricating pillars by molding.^[135]

Table 2 illustrates the basic working principles and specifications of fabrication methods for 2D structures, extruded in the third dimension with a fixed extrusion height or depth (geometric complexity level 1).

3. Fabrication Methods for 3D Structures with Areas of Various Heights and No Overhanging Parts or Cavities (Geometric Complexity Level 2)

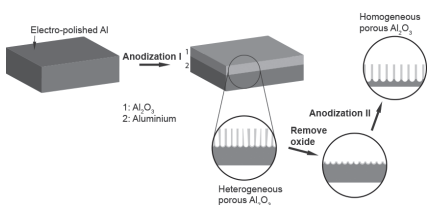
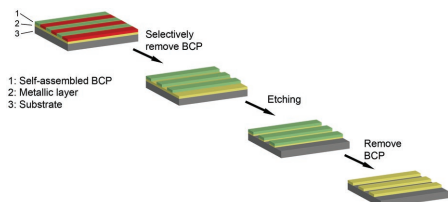
3D structures with areas of various heights but without overhanging parts or cavities can be fabricated with droplet deposition

Table 2. Fabrication methods for two-dimensional structures extruded in the third dimension with a fixed extrusion height or depth (geometric complexity level 1).

Fabrication method	Material complexity	Resolution	Total size	Geometric diversity	Materials diversity	Throughput
<p>Scanning probe lithography (SPL)</p> <p>Substrate, Scanning probe, Ink, Resist layer (e.g., thermo-responsive polymer), Heated scanning probe</p> <p>Additive SPL (DPN) Subtractive SPL (thermal SPL)</p>	Multiple materials possible	10 nm ^[63]	Up to 500 μm ² ^[61]	Two tunable dimensions	Multiple materials possible: Biomaterials, soft matter, nanoparticles, graphene, silicon, ceramics, etc.	Low
<p>Photolithography</p> <p>Photo-mask, UV Light, Etching, Etching</p> <p>1: Photoresist layer 2: Metallic layer 3: Substrate</p> <p>Photoresist selectively removed Photoresist and exposed regions in metallic layer removed</p>	Multiple materials possible	Down to 37 nm; ^[83] potentially sub-10 nm ^[87]	15 cm diameter circular substrates	Two tunable dimensions	Only photosensitive materials	Very high
<p>Scanning beam lithography: Optical beam lithography (OBL)</p> <p>Laser beam, Resist layer, Substrate, Photopolymer</p> <p>Subtractive OBL: excitation Additive OBL: photopolymerization</p>	Single material structures	52 nm ^[34]	2 × 2 cm ² substrates ^[45]	Three tunable dimensions	Only photosensitive materials	Low
<p>Scanning beam lithography: Ion beam lithography (IBL)</p> <p>FIB, Sputtered atoms, Resist layer, Resist layer, Implanted atoms</p> <p>Milling/Sputtering/Writing Chemical modification/implantation</p>	Single material structures	8 nm ^[107]	12.5 × 12.5 mm ² pillar arrays; ^[90] centimeter-sized patterns ^[105]	Two tunable dimensions	Polymeric or metallic materials	Low
<p>Scanning beam lithography: Electron beam lithography (EBL)</p> <p>Electron beam, Resist layer, Substrate</p> <p>Milling Chemical modification</p>	Single material structures	4 nm ^[104]	Wafers and photomasks up to around 30 cm diameter ^[78]	Two tunable dimensions	Polymeric or metallic materials	Low
<p>Directed self-assembly of planar 2D structures: Colloidal lithography</p> <p>Precipitate colloids, Etching/Deposition, Remove or dissolve colloids</p> <p>1: Metal/Polymer layer 2: Substrate</p>	Single material structures	Down to tens of nm	Up to 15 cm (6 in.) diameter substrates ^[136]	Two tunable dimensions	Polymeric or metallic materials	Medium

Table 2. Continued.

Fabrication method	Material complexity	Resolution	Total size	Geometric diversity	Materials diversity	Throughput
Directed self-assembly of planar 2D structures: Block-copolymer (BCP) lithography	Single material-structures	6 nm ^[117]	300 mm diameter wafers ^[137]	Two tunable dimensions	Polymeric or metallic materials	Medium
Directed self-assembly of planar 2D structures: Nanoporous anodic aluminum oxide (AAO)	Single material structures	10–450 nm ^[134]	1 cm ²	Two tunable dimensions	Only aluminum oxide	Low



methods and molding techniques. In this section, droplet deposition methods (electrohydrodynamic jet printing and laser-induced forward transfer (LIFT)), hard molding (nanoimprint lithography (NIL) and step-and-flash imprint lithography (SFIL)), and soft molding (replica molding, microtransfer molding, micromolding in capillaries, solvent-assisted micromolding, microcontact printing, and nanotransfer patterning) techniques are reviewed.

3.1. Droplet Deposition Methods

Droplet deposition methods are methods in which structures are formed out of liquid droplets of, for example, metals or particle solutions. Structures are built from fusion of droplets by melting or flowing upon deposition. Droplet deposition methods are mainly used for depositing 2D patterns, resulting in structures of level-2 geometric complexity. 3D structures can be fabricated in a layer-by-layer fashion, or in a sequential fashion to create, for example, wire-like structures.^[138] The attainable resolution of droplet-printing methods is limited by the droplet size, which is typically in the order of 100 nm.^[138] Droplet printing methods have a serial character in all three dimensions, as opposed to scanning beam methods, where the pattern height or depth is developed simultaneously with the 2D patterning. Therefore, droplet-printing methods are relatively slow. Here, we discuss electro-hydrodynamic jet printing and laser-induced forward transfer.

3.1.1. Electro-Hydrodynamic Jet Printing

In EHD jet printing, microdroplets of nanoparticles, polymers, and proteins are used to print patterns on a substrate.

The ink microdroplets are created by applying an electric potential over a larger ink droplet ejected through a nozzle, causing mobile ions to accumulate at the nozzle tip and to form a pulsating droplet, which is called a Taylor cone.^[19] By controlling the electric field strength, streams of droplets much smaller than the nozzle diameter can be formed. The resolution of EHD improves with a decreasing size of the jetted microdroplets, for example, by optimizing the Taylor cone using viscoelastic inks,^[139] and with increasing microdroplet placement accuracy. Accuracy of microdroplet placement can be increased by lowering the distance between the nozzle and the substrate^[19] or by surface functionalization, in which case the positioning of the microdroplets is controlled by regions of varying wettability or by relief on the surface.^[140] A maximum positioning accuracy around 10 μm has been reported.^[140] Feature sizes down to 240 nm with a nozzle diameter of 300 nm were achieved by Park et al.^[140] by dissolving 3 nm sized nanoparticles in microdroplets. Upon evaporation of the microdroplet, nanoparticle deposits were obtained. With EHD, it is possible to print more than one material in one structure. For example, Sutanto et al.^[141] used organic silver ink to print conductive lines, with photocurable polymer prints as an isolator between the conductive lines.

3.1.2. Laser-Induced Forward Transfer

In LIFT, metal droplets are transferred to a substrate from a so-called donor layer. This layer has a thickness of about 100 nm and is positioned at about 100 μm from the substrate. The donor layer is supported by a transparent carrying layer, and upon selective exposure to a pulsed laser, local evaporation of the donor layer results in ejection of microdroplets, which

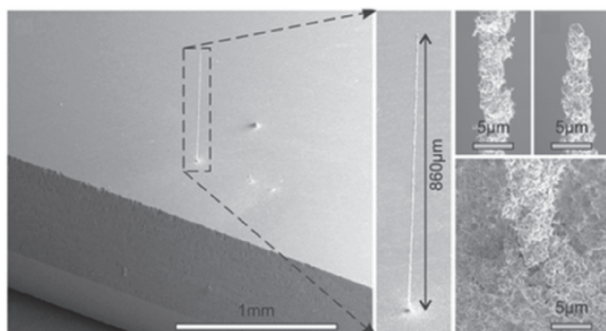


Figure 6. Left: A high-aspect ratio pillar fabricated with laser-induced forward transfer. Middle: A close-up of the same pillar. Top right: The thickness of the pillar at its center and top is about 4 μm . Bottom right: The thickness of the pillar at its base is 6 μm , because of multiple droplets being deposited close to the pillar. Adapted with permission.^[142] Copyright 2015, John Wiley and Sons.

are captured by the substrate.^[142] Metals that are used in LIFT include chromium, tungsten, gold, nickel, and aluminum; also pastes, hydrogels, and liquids are used in LIFT methods.^[142] Because the droplets melt together upon deposition, structures fabricated with LIFT are relative inhomogeneous. The droplet size depends on the size of the focal point of the laser, and thus the exposed area on the donor layer.^[143] Layers with a thickness of 3.5 μm have been fabricated.^[143] Moreover, high aspect-ratio pillars (5 μm in diameter, 860 μm in height) have been fabricated by stacking of droplets (**Figure 6**).^[142] Since droplets are deposited in vertical direction, overhanging structures cannot be printed in principle, although some metallic droplets, when molten together, do provide sufficient mechanical strength to realize overhanging structures.^[144]

3.2. Imprinting with Hard Molds

In imprinting methods, a 3D template (referred to as mold) is used to press a pattern into a layer located on a substrate. The shaped layer is commonly referred to as the resist layer. If the resist layer is heated before imprinting, these methods are sometimes called hot embossing.^[145] Hard molds are usually fabricated by means of SBL and typically made of quartz or silica, because these materials are chemically inert to most monomers and (pre)polymers.^[23] Moreover, because of the low thermal expansion coefficients of quartz and silica, hard molds are compatible with manufacturing processes that require high temperatures.^[146]

Forming nanostructures or microstructures in a resist layer with the use of a hard mold is a contact process and therefore comes with specific challenges. The pressure on the resist needs to be uniformly distributed during molding, which is facilitated by the residual layer, the compressed layer of resist that prevents the mold from making contact with the underlying substrate. Removing the residual layer after molding requires a subsequent etching step of the molded structure.^[147] Defect control during release of the mold is also a challenge, commonly tackled by pre-coating the mold with a release layer.^[148,149]

With imprinting methods, the fabricated structure is freely tunable in one dimension, because the imprint depth or the

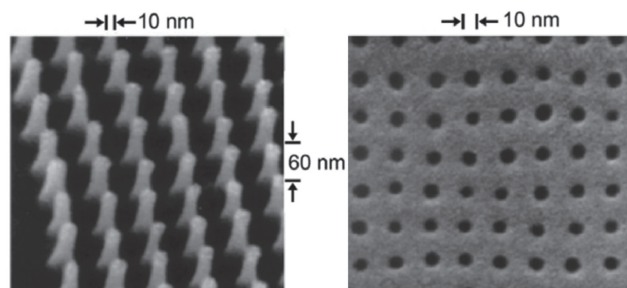


Figure 7. A silica mold (left), used to imprint a polydimethylsiloxane layer (right). The holes are 10 nm wide; the spacing is 40 nm. Reproduced with permission.^[25] Copyright 1997, AIP Publishing.

thickness of the deposited layer can be freely tuned. Because a full 2D pattern is imprinted in a parallel fashion, the throughput of imprinting methods is in the order of $10^{-4} \text{ m}^2 \text{ h}^{-1}$, which is typically higher than most serial methods.^[19] Hard molding methods can be divided in NIL and SFIL, which both will be discussed here.

3.2.1. Nanoimprint Lithography

In NIL, a mold is used to shape a polymer glass when above the transition temperature T_g of the polymer. Upon cooling down, the polymer hardens, and the template is removed, leaving the patterned resist.^[46] The patterned layer can be the final nanostructure or can act as an etch-resistant layer in a subsequent etching step. NIL, sometimes referred to as thermal NIL, was introduced in 1995,^[46,150] and exceptionally low feature sizes (about 10 nm) were demonstrated soon after that.^[25] Therefore, and because of limited instrumental requirements and a high-throughput, NIL quickly became a serious contender of conventional nanofabrication methods such as photolithography and EBL.^[149] To increase the throughput of NIL, the use of a rolling pin-like mold was suggested in 2008,^[151] in which a flexible oblong substrate is guided over a rotating cylindrical mold. NIL has been used to make soft molds or stamps,^[152] high aspect ratio parallel lines on a substrate,^[149] nanopillars,^[153] and microfluidic devices.^[154] A silica mold with 10 nm wide pillars, separated by 40 nm spacing, was fabricated to imprint a polydimethylsiloxane (PDMS) layer (**Figure 7**), resulting in similar sized holes.^[25] High aspect ratios of about 20 have been also reported.^[155] NIL is often used as part of a fabrication toolbox set, for example, for fabricating the master structure in a replication molding process.^[148]

3.2.2. Step-and-Flash Imprint Lithography

In SFIL (sometimes referred to as UV-NIL),^[149] UV light is used to polymerize a photosensitive prepolymer during molding. The mold has thus to be transparent, made of, for example, quartz or silica.^[146] SFIL is more suitable than NIL for fabricating structures consisting of multiple stacked layers, because, due to the transparency of the mold, layer alignment is easier with SFIL. Furthermore, because of the milder molding conditions of SFIL, the shaped layers do not need to

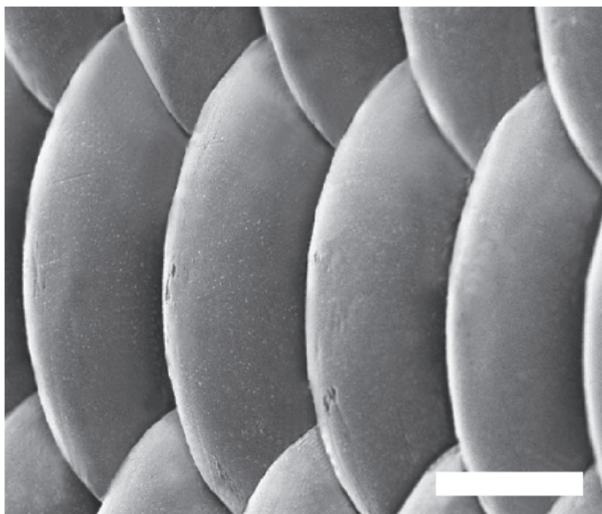


Figure 8. Replicated microlenses, fabricated with a two-step SFIL process. A negative replica of the master mold was obtained by imprinting a UV-curable resist. Upon application of a release layer, this negative replica was used in a second imprinting step to obtain the replicated microlenses. Scale bar is 10 μm . Adapted with permission.^[158] Copyright 2018, Springer Berlin Heidelberg.

undergo large temperature changes for each subsequent layer, as is the case with NIL.^[23,156] Photocurable low-viscous acrylate-based precursors^[157] and biomaterials^[24] can be used as resists. SFIL has also been used in two-step imprinting processes to replicate complex structures (**Figure 8**).^[158] With SFIL, lines of 20 nm width have been fabricated, as well as multilayered structures.^[159] Even 4 nm line widths were demonstrated by imprinting an ion-beam fabricated pattern of HSQ into a PDMS-based UV resist.^[160] A method similar to SFIL is jet-and-flash imprint lithography, in which the resist layer is jetted on a substrate.^[24]

3.3. Shaping and Printing with Soft Molds

Fabrication methods in which soft molds are used for shaping, printing, or pattern transfer are generally referred to as soft lithography. Soft molding methods were introduced in the late 1990s^[161–164] and rapidly became popular for research purposes, because, contrary to hard molds, soft molds are inexpensive to make. Soft molds are often made of PDMS, a polymer that is deformable, inexpensive, inert to most chemical solvents, and easy to process.^[23] A wide range of materials can be used as resist, varying from amorphous, thermoplastic, and crystalline polymers to gels, ceramics, lithographic resists, and even paper, creating biobased microstructures. Some resists need subsequent curing, for example, by inducing crosslinking or by changing the temperature.^[23] Mechanical properties, friction between mold and resist, transparency, chemical inertness, and costs are some of the main criteria for choosing the resist material.^[165]

Contrary to hard molds, which can only be used on planar substrates, soft molds can be also used on nonplanar substrates. When shaping a deformable layer with a 3D mold,

the geometric diversity is low (i.e., no tunable dimensions), because only the specific geometry of the used mold can be fabricated. When a (soft) mold is used for stamping, imprinting, or printing, the thickness (or depth) of the deposited (or imprinted) pattern is tunable, so the geometric diversity that can be attained with these methods is higher compared to using mold for shaping a resist layer.

Here, we discuss shaping methods (including microtransfer molding, micromolding in capillaries, solvent-assisted micromolding, and replica molding) and printing methods (including microcontact printing and nanotransfer printing methods).

3.3.1. Shaping Methods with Soft Molds

Soft molds are commonly used to shape or pattern deformable polymeric layers. This is done either by filling the mold or by pressing the mold into the layer. Microtransfer molding (μTM) is a method in which a soft mold is used to first fabricate a pattern from curing a shaped liquid precursor, and then transfer it to a substrate. With μTM , the smallest attainable feature sizes are about 100 nm, a limit caused by the fact that smaller (negative) features in the mold are too small for the liquid to fill them. In principle, with μTM (and molding methods in general) only level-2 complexity structures can be fabricated, as overhanging structures cannot be decasted from a 3D mold. However, LaFratta et al.^[166] used μTM to fabricate acrylic replicas of masters with overhanging features (**Figure 9**), by exploiting the deformability of the mold, which allowed mold removal by means of stretching after transfer to a glass substrate. In a method similar to μTM , Hamedi et al.^[17] used 3D-printed PU molds to shape paper, which was subsequently assembled to form disposable paper-based micro-channel structures.

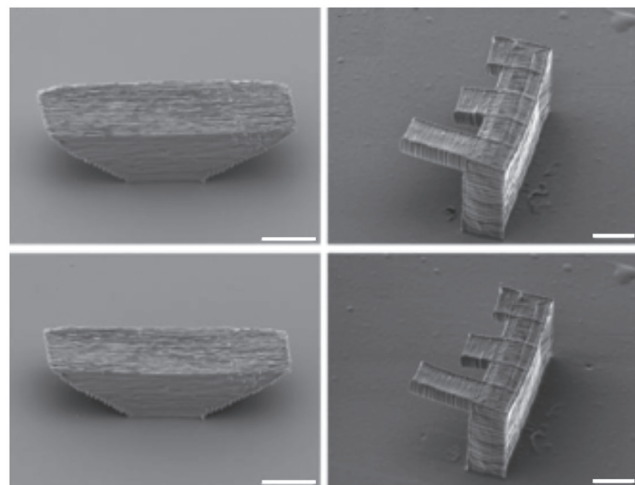


Figure 9. Master structures (top), on which PDMS is casted to create an elastomeric mold. This mold is then filled with an acrylic resin, which is subsequently transferred to a glass substrate. These structures have an overhang of around 10 μm , but still replicas can be fabricated because the molds are stretchable (bottom). The scale bars are 10 μm . Adapted with permission.^[166] Copyright 2004, American Chemical Society.

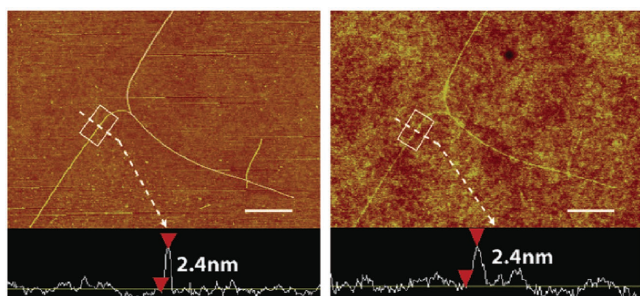


Figure 10. Left: Carbon single-walled nanotubes on a silica substrate. By casting and curing polydimethylsiloxane on the substrate, a mold is obtained with feature sizes below 1 nm. Right: Replicated single-walled nanotubes, fabricated by shaping a polyurethane layer using the obtained PDMS mold. The scale bars are 1 μm . Adapted with permission.^[172] Copyright 2004, American Chemical Society.

To fill nanoscale and microscale features of a soft mold with a liquid prepolymer resist, capillary action can be used. This method is referred to as micromolding in capillaries. After a droplet of prepolymer is dragged into the mold (sometimes facilitated by a pressure difference over the capillaries,^[167] by heating the prepolymer,^[168] or by an electric field^[23]), the polymer resist is hardened by means of solvent evaporation. Due to flow resistance, the smallest attainable feature size is around 100 nm.^[23]

Another way to facilitate mold filling is by wetting the mold with a good solvent for the polymeric resist. Upon contact with the mold, the polymer softens and conforms to the mold. Hardening of the polymer is achieved by letting the solvent dissipate and evaporate into the PDMS mold. This strategy of mold filling is referred to as solvent-assisted micromolding (SAMIM).^[23] Because no high temperature is required during the SAMIM process, disadvantageous effects such as shrinkage after cooling, polymer degradation at high temperatures, and incompatibility with high- T_g materials do not play a role in SAMIM.^[169] Parallel lines with a width of around 60 nm have been achieved with this method,^[162] although resolutions are typically in the order of micrometers.^[170,171]

Replica molding (RM) is a technique in which a hard mold or pattern (the so-called master) is replicated using soft molds.^[163,172] In RM, first PDMS is casted on the master, which is then cured to obtain a negative pattern. This negative pattern is subsequently used as a template for the replica by means of shaping a PDMS resist layer on a substrate. The negative PDMS patterns are inexpensive to fabricate and reusable. RM has been used to replicate SWNTs on a substrate, down to feature sizes of 1 nm (Figure 10).^[172] A bilayer of PDMS (one soft and one hard layer) was needed to protect the SWNTs from getting damaged and still get a robust PDMS imprint. Also nanorods with a diameter of 30–150 nm have been successfully replicated.^[173] RM has been further used to fabricate biomimetic adhering surfaces, consisting of pillar arrays, to study the interlocking of two approaching surfaces.^[174]

3.3.2. Printing and Pattern Transfer Methods with Soft Molds

Soft molds are also used to transfer an ink to a substrate, a method referred to as printing. In microcontact printing (μCP),

a coating (e.g., alkanethiols)^[175] is selectively transferred from an elastomeric stamp to a substrate. The transferred coating thus acts as an ink and is only transferred upon contact with the substrate, because it is functionalized with a thin layer of a noble metal. The ink is transferred by diffusion and covalent-bond formation with the metal layer, requiring molecular-scale contact between the stamp and the substrate. The transferred ink then self-assembles into a monolayer.^[176] With μCP , printed features can be as small as the stamp allows, and feature sizes down to 50 nm have been reported.^[177] Besides printing self-assembling monolayers, also biomolecules^[178] and nanoparticles^[179] can be selectively deposited on substrates, which is useful in cell patterning. Deposited ink can also act as a positive or negative resist in a subsequent etching step.^[180] Choi et al.^[181] demonstrated multiple-layer transfer printing to create arrays of micrometer-sized light-emitting diodes. To increase the material diversity of inks compatible with μCP , Li et al.^[182] suggested the use of molds, the surface energy of which can be controlled. By chemically modifying polyurethane acrylate based molds, the release and transfer of printed materials is optimized.

Similar to μCP is nanotransfer patterning (nTP), in which a thin film of, for example, polymers^[183] is transferred from a hard or soft stamp to a substrate. This thin film has the 3D shape of the used stamp. Pattern transfer takes place by covalent or noncovalent interactions between substrate and pattern. The resolution of nTP is limited by the resolution of the elastomeric stamp and by the materials used for the mold and resist. Lines of 8 nm width have been shown when a soft stamp (made of directed self-assembled BCPs on a substrate) was inked with gold and this ink was transferred to a PDMS substrate by covalent bond formation.^[183]

Table 3 illustrates the basic working principles and specifications of fabrication methods for 3D structures with areas of various heights and no overhanging parts or cavities (geometric complexity level 2).

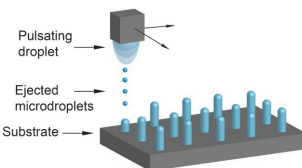
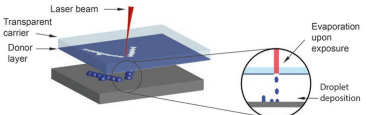
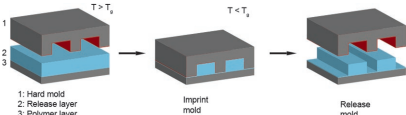
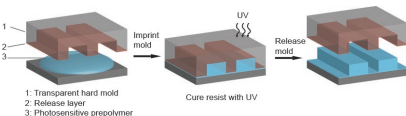
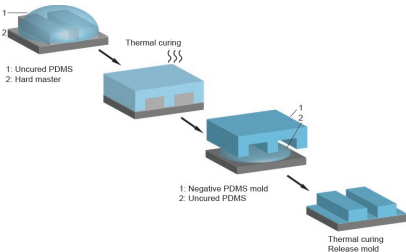
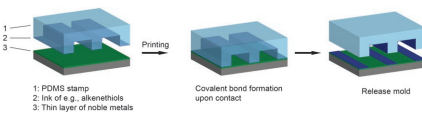
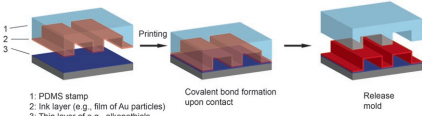
4. Fabrication Methods for 3D Structures with Overhanging Features and/or Cavities (Geometric Complexity Level 3)

In this section, we discuss nanofabrication and microfabrication methods in which structures can be fabricated in a 3D direct-writing fashion: vat photopolymerization (stereolithography (SL) and direct laser writing (DLW)), focused ion or electron beam-induced deposition, and directed self-assembly. These fabrication methods are all serial, additive methods, meaning that the structure is fabricated voxel by voxel, and complex structures with overhanging features and cavities can be fabricated.

4.1. Vat Photopolymerization

Vat photopolymerization is a collective name for fabrication methods in which nanostructures or microstructures are formed by curing a liquid photoresist (also referred to as a resin) in a vat. Curing of the resin takes place at the focal point of a laser beam, and by controlling the position of this focal point (including the depth), 3D structures can be fabricated. Resins

Table 3. Fabrication methods for 3D structures with areas of various heights and no overhanging parts or cavities (geometric complexity level 2).

Fabrication methods	Material complexity	Resolution	Total size	Geometric diversity	Material diversity	Throughput
<p>Electro-hydrodynamic jet printing (EHD)</p> 	Multiple materials possible	240 nm (using evaporation of deposited droplets) ^[140]	15 × 15 μm ² with BCPs; ^[116] several mm ² with polymeric particles ^[140]	Two tunable dimensions (extrusion in third dimension possible)	Multiple materials possible: polymers, biomaterials	Low
<p>Laser-induced forward transfer (LIFT)</p> 	Single material structures	Down to 3.5 μm ^[143]	Not reported	Two tunable dimensions	Only metallic materials	Low
<p>Hard molding: Nanoimprint lithography (NIL)</p> 	Single material structures	30 nm ^[155]	300 × 400 mm ² ^[184]	One tunable dimension	Only polymeric materials	High
<p>Hard molding: Step-and-flash imprint lithography (SFIL)</p> 	Single material structures	5 nm ^[24]	Up to 250 × 250 mm ² wafers ^[185]	One tunable dimension	Only polymeric materials	High
<p>Soft molding: Replica molding</p> 	Single material structures	3 nm ^[172]	100 mm ²	Zero tunable dimensions	Multiple materials possible: biomaterials, elastomers, paper	Soft mold: 100 mm ² per cycle ^[186]
<p>Soft molding: Microcontact printing (μCP)</p> 	Multiple materials possible	50 nm ^[177]	A few cm ² ^[177]	Zero tunable dimensions (one tunable dimension in a layer-by-layer fashion)	Multiple materials possible: biomaterials, elastomers, etc.	High
<p>Soft molding: Nanotransfer patterning (nTP)</p> 	Multiple materials possible	8 nm ^[183]	100 mm diameter substrates ^[183]	Zero tunable dimensions	Multiple materials: Biomaterials, elastomers, etc.	High

compatible with vat photopolymerization include photopolymers, but also collagen-hydrogel has been used.^[187] No multimaterial structures can be fabricated, as the vat can be filled only with one type of resin. The photosensitivity of the resin needs

to be high, such that polymerization only takes place locally, and not in neighboring regions.^[85] The resolution is determined by the size of the focal point. To reduce the focal point size, stimulated emission depletion (STED) methods are used in vat

photopolymerization,^[188,189] where a second beam acts as an inhibitor of the writing beam by creating destructive interference pattern at the peripheral regions of the focal point. Another approach to obtain high resolutions with optical-beam fabrication methods for 3D structures is the use of a spatial light modulator, in which the focal point shape is spatially tuned by electronic modulation, varying wave front, intensity, or polarization of the laser beam.^[189,190] With vat photopolymerization methods, high geometric diversity can be obtained, because fabricated structures are tunable in all three dimensions. Because of its serial character, vat photopolymerization is not a very fast technique, with scanning speeds in the order of micrometers per second.^[19]

4.1.1. Stereolithography

SL is a vat photopolymerization method in which a laser beam serially solidifies the resin by means of photopolymerization. The resin consists of liquid photopolymer, sometimes with a photoinitiator, which starts the polymerization upon light exposure. The vat with the resin is moved around a stable focal point of a laser. By means of polymerization, the structure is formed point-by-point and layer-by-layer.^[31] The minimal layer thickness in SL is determined by the volume of the focal point (and thus by the polymerization volume), the resin viscosity, and the surface tension of the resin. Resolutions in the μm -range were obtained soon after the introduction of SL as a fabrication method.^[191] SL is used in various fields, including the fabrication of micromachines,^[192] microfluidic systems,^[193] tissue engineering,^[187] and bioanalysis.^[31]

4.1.2. Direct Laser Writing

DLW is a vat photopolymerization technique in which the process of two-photon-polymerization (TPP, also abbreviated as 2PP) or multiphoton-polymerization (MPP) is applied to obtain smaller polymerization volumes within the laser beam focal point compared to SL. TPP and MPP rely on the fact that the resin polymerizes only when two or more photons are absorbed simultaneously. Polymerization therefore only takes place in the center of the focal point, where the photon intensity is sufficiently high for this simultaneous absorption to occur, thereby reducing the polymerization volume.^[194] TPP was introduced in resin-based AM in 1990,^[195] and with the ongoing progress of optics and resists, diverse structures have been fabricated with it. In **Figure 11**, three examples of structures with feature sizes below $1\ \mu\text{m}$ are shown, fabricated with a commercial instrument and resist, using a 405 nm diode laser.^[196] With this setup, linewidths down to 78 nm and point diameters down to 50–70 nm have been demonstrated.^[196] With STED-based DLW, resolutions down to 100 nm have been reported.^[197] DLW has also been used to fabricate biocompatible porous scaffolds to grow cells in.^[198] Also for bioinspired adhesive or (de)wetting surfaces, which are commonly fabricated with lithographic methods,^[4,199] DLW methods have been used, because of the attainable high resolutions in combination with geometric diversity. An example of a bioinspired surface with variable wetting properties to water was fabricated by Tricinci et al.,^[60] who used DLW with an epoxy-based resist to write an array of

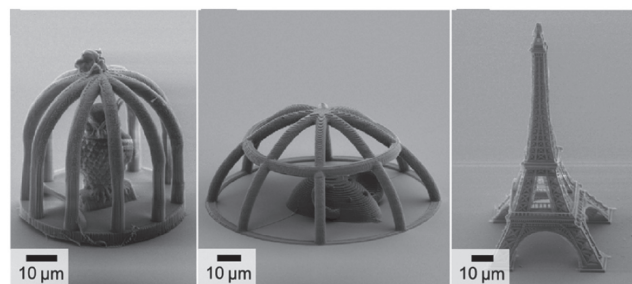


Figure 11. Microstructures fabricated with DLW in a commercially available photoresist. Reproduced with permission.^[196] Copyright 2014, Optical Society of America.

tree-like structures, similar to the pattern on the leaves of *Salvinia molesta* (see **Figure 12**).

The terminology of resin-based AM methods varies in the literature. DLW methods are also referred to as 3D OBL,^[34] laser 3D printing,^[198] and direct laser lithography.^[60] DLW is also called TPP, 2PP, MPP, nonlinear lithography, and multiphoton lithography.^[194] Sometimes, TPP methods are considered as a special stereolithography technique, and referred to as micro-SL^[31] or TPP-SL.^[200]

4.2. Focused Ion or Electron Beam-Induced Deposition

Focused ion beam-induced deposition (FIBID) and focused electron beam-induced deposition (FEBID) are nanolithographic direct-writing fabrication methods in which a beam of ions or electrons is used to induce molecular decomposition of a gas (commonly metal–organic molecules), resulting in local chemical vapor deposition on a substrate.^[201,202] Deposition of materials is limited to one material at a time. FIBID and FEBID are suitable for fabrication of 3D structures, because deposition can be controlled precisely by tuning the beam diameter and its focal point. With FIBID, spirals with a wire thickness of about 80 nm have been fabricated by means of platinum deposition (**Figure 13**).^[203] FEBID is used for lithographic mask repair, probe preparation in SPL methods, and fabrication of nanotubes.^[202,204]

Deposition of particles from a gas can also be induced by a laser beam. This technique is referred to as laser chemical

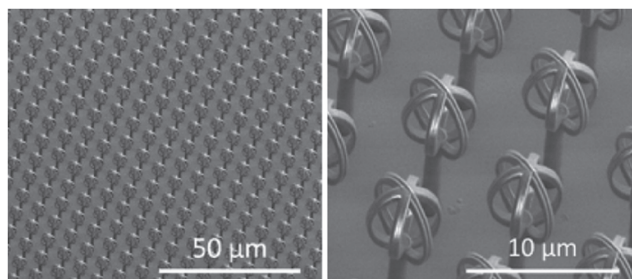


Figure 12. Inspired by the *Salvinia molesta* leaf, patterns were fabricated that, when submerged in water, trap a layer of air. One module of this repetitive microstructure consists of a $7\ \mu\text{m}$ tall hair (diameter of $1.5\ \mu\text{m}$), with three intersecting circles (diameter of $6\ \mu\text{m}$) as a head. The structures were written in an epoxy-based resist, using DLW. Reproduced with permission.^[60] Copyright 2015, American Chemical Society.

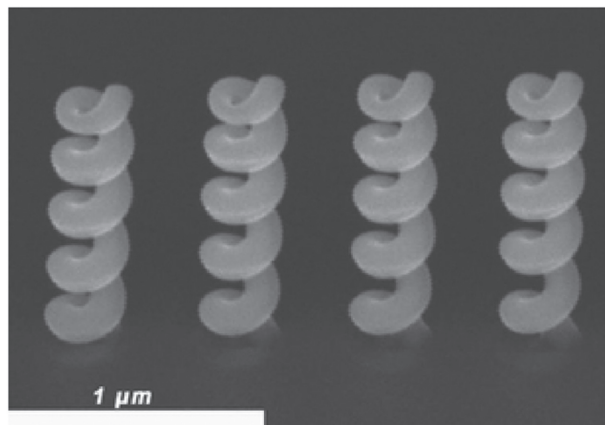


Figure 13. Platinum nanospirals fabricated with focused ion beam-induced deposition on a Si substrate. Because the presence of the first nanospiral changes the particle scattering behavior, the second and next nanospirals have a different growth rate during fabrication compared to the first one. Adapted with permission.^[203] Copyright 2014, John Wiley and Sons.

vapor deposition.^[31] The focal point has a diameter of about 1 μm , meaning that attainable resolutions are lower than those attained with FIBID and FEBID.

4.3. Directed Self-Assembly of 3D Structures

Besides using macromolecules as building blocks for single-layer patterns on planar substrates, as is done with BCP lithography and colloidal lithography, self-assembling macromolecules can also be used to fabricate 3D structures.^[205] The self-assembling properties can be tailored by tuning the dissolvability, the functional groups, or the molecular size of the macromolecules.

Inspired by cells and their organelles, a range of vesicles and nanospheres have been fabricated by exploiting the physical properties of macromolecules. These nanospheres can be used as microreactors^[206] or drug carriers.^[207] Amphiphilic polymers have been applied as building blocks for functional membranes, which can be used for separation processes (e.g., osmosis, filtration) or catalysis.^[208] Macromolecules have been also used as building blocks for stimuli-responsive structures, like spheres or surfaces.^[209] Akerboom et al.^[210] fabricated surfaces with controllable wettability using an array of self-assembled carboxylated polystyrene colloids as templates. By dissolving the colloid array after casting polypyrrole on the top of the array, air-filled cavities in a polypyrrole surface were fabricated (see **Figure 14**).

Table 4 illustrates the basic working principles and specifications of fabrication methods for 3D structures containing cavities and/or overhanging features (geometric complexity level 3).

5. Discussion

In this paper, we reviewed nanofabrication and microfabrication methods using seven moderators related to the characteristics of the envisioned structures, namely geometric complexity, material complexity, resolution, total size, geometric diversity,

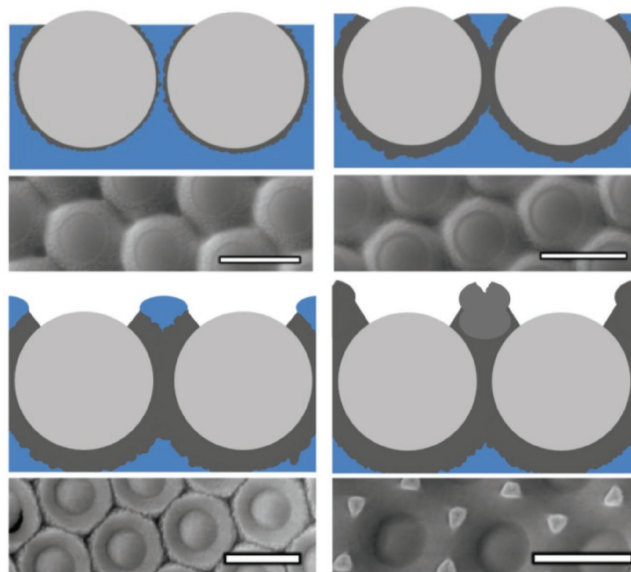


Figure 14. Overhanging features fabricated by polymerizing pyrrole monomers around a monolayer of carboxylated polystyrene colloids (grey spheres) at the air–water interface. Subsequent dissolving of the colloidal template resulted in a polypyrrole crystalline structure. Adapted with permission.^[210] Copyright 2015, American Chemical Society.

material diversity, and throughput. Ten groups of fabrication methods were identified, and their working mechanisms and specifications were reviewed.

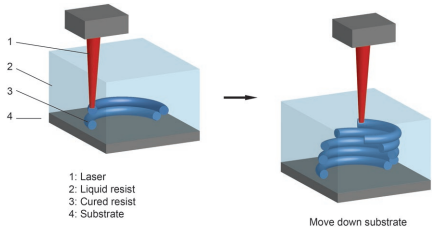
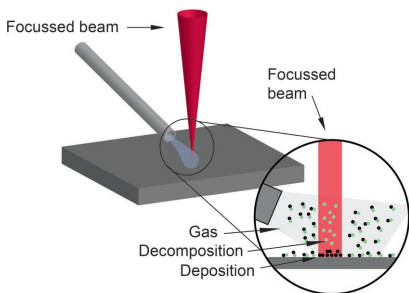
5.1. Choosing between Fabrication Methods: A Multivariate Problem

When fabricating a nanostructure or microstructure, choosing the most suitable fabrication method to realize the envisioned performance is a multivariate problem. To facilitate this decision-making process, **Figure 15** and **Table 5** can be used. Figure 15 illustrates the aforementioned seven moderators in a radar plot for the ten groups of nanofabrication and microfabrication methods discussed in this paper. For each of the moderators in the radar plot, we show typical values, rather than absolute limits. For example, we classify the resolution of self-assembly methods in the 11–100 nm range, although resolutions of 6 nm have been also reported.^[117]

The radar plot lends itself to several observations and trends:

- (1) Photolithography is characterized by relatively high resolution and throughputs. While with other serial lithographic methods (SBL and FIBID/FEBID) high resolutions can be also obtained, the throughput of these methods is lower than that of photolithography, which may explain why photolithography rather than other serial lithographic methods is a preferred method in industrial-scale applications.
- (2) Hard molding achieves structures of larger total size than soft molding. With relatively high throughput, hard molding can be useful for industrial purposes, whereas soft molding is popular in research, as it is quite fast and relatively high resolutions can be obtained with it.

Table 4. Fabrication methods for 3D structures containing cavities and/or overhanging features (geometric complexity level 3).

Fabrication methods	Material complexity	Resolution	Total size	Geometric diversity	Material diversity	Throughput
<p>Vat photopolymerization</p>  <p>1: Laser 2: Liquid resist 3: Cured resist 4: Substrate</p> <p>Move down substrate</p>	Single material structures	0.1–10 μm ^[31,203]	100 μm ^[85]	Three tunable dimensions	Only photosensitive materials	Low
<p>Focused ion or electron beam-induced deposition</p>  <p>Focussed beam</p> <p>Focussed beam</p> <p>Gas Decomposition Deposition</p>	Single material materials	100 nm ^[201,203]	300 mm sized wafers	Three tunable dimensions	Limited to metal–organic gases	Low

- (3) SPL has low throughputs and attainable complexity, but the method is compatible with a wide range of materials due to its mild processing conditions. Furthermore, with SPL the highest resolutions can be obtained, down to features on single-molecule length scales.
- (4) Nanodroplet and microdroplet deposition methods such as LIFT or EHD exhibit advantages from a structural

- perspective, as they can be used to fabricate structures with a large total size with high complexity and diversity. Due to the serial character of fabricating, however, throughput is low, and resolutions are limited at the micrometer range.
- (5) The highest geometric complexity can be obtained with vat photopolymerization. On the other hand, the resin in vat photopolymerization needs to be a photocurable material,

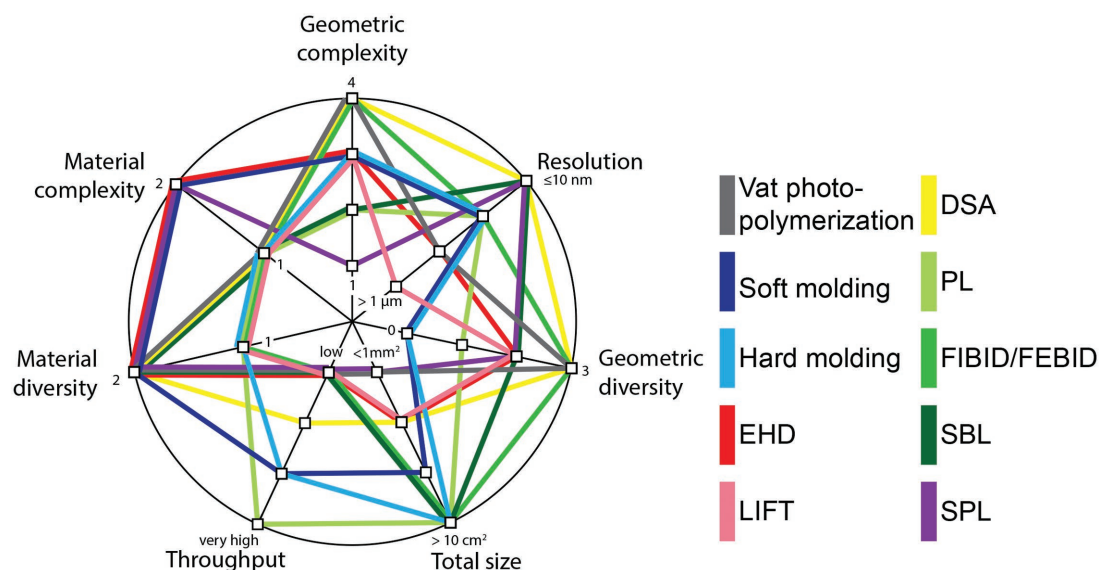


Figure 15. Performance of ten groups of nanofabrication and microfabrication methods in terms of geometric complexity (levels 1–3), resolution ($>1\ \mu\text{m}$, $101\ \text{nm}$ – $1\ \mu\text{m}$, 11 – $100\ \text{nm}$, and $\leq 10\ \text{nm}$), geometric diversity (0–3 tunable dimensions), total size of the structure ($<1\ \text{mm}^2$, 1 – $99\ \text{mm}^2$, 1 – $10\ \text{cm}^2$, and $>10\ \text{cm}^2$), throughput (low, medium, high, and very high), material diversity (one group of materials or multiple groups of materials), and material complexity (one group of materials or multiple groups of materials). All ranges are described from the origin to the outer circle.

Table 5. Performance of ten groups of nanofabrication and microfabrication methods in terms of seven moderators.

Geometric complexity	Level 1	Level 2	Level 3	Level 4
	Scanning probe lithography (SPL)	Photolithography Scanning beam lithography (SBL)	Soft molding Hard molding Electrohydrodynamic jet printing (EHD) Laser-induced forward transfer (LIFT)	Directed self-assembly (DSA) Vat photopolymerization Focus ion/electron beam-induced deposition (FIBID/FEBID)
Material complexity	Single		Multiple	
	Vat photopolymerization Hard molding Laser-induced forward transfer (LIFT) FIBID/FEBID	Directed self-assembly (DSA) Photolithography Scanning beam lithography (SBL)	Electrohydrodynamic jet printing (EHD) Soft molding Scanning probe lithography (SPL)	
Resolution	≤10 nm	11–100 nm	101 nm ⁻¹ μm	>1 μm
	Directed self-assembly (DSA) Scanning beam lithography (SBL) Scanning probe lithography (SPL)	Soft molding Hard molding Focus ion/electron beam-induced deposition (FIBID/FEBID) Photolithography	Electrohydrodynamic jet printing (EHD) Vat photopolymerization	Laser-induced forward transfer (LIFT)
Total size	<1 mm ²	1–99 mm ²	1–10 cm ²	>10 cm ²
	Vat photopolymerization Scanning probe lithography (SPL)	Electrohydrodynamic jet printing (EHD) Laser-induced forward transfer (LIFT) Directed self-assembly (DSA)	Soft molding	Photolithography Scanning beam lithography (SBL) Hard molding Focus ion/electron beam-induced deposition (FIBID/FEBID)
Geometric diversity	0D	1D	2D	3D
	Soft molding Hard molding	Photolithography	Scanning beam lithography Electrohydrodynamic jet printing (EHD) Laser-induced forward transfer (LIFT) Scanning probe lithography (SPL)	Focus ion/electron beam-induced deposition (FIBID/FEBID) Directed self-assembly (DSA) Vat photopolymerization
Material diversity	Single		Multiple	
	Laser-induced forward transfer (LIFT) Hard molding	Photolithography Focus ion/electron beam-induced deposition (FIBID/FEBID)	Electrohydrodynamic jet printing (EHD) Scanning probe lithography (SPL) Vat photopolymerization	Directed self-assembly (DSA) Scanning beam lithography (SBL) Soft molding
Throughput	Low	Medium	High	Very high
	Scanning beam lithography (SBL) Scanning probe lithography (SPL) Laser-induced forward transfer (LIFT) Electrohydrodynamic jet printing (EHD) Focus ion/electron beam-induced deposition (FIBID/FEBID) Vat photopolymerization	Directed self-assembly (DSA)	Soft molding Hard molding	Photolithography

which limits the range of compatible materials. With vat photopolymerization, also high resolutions can be obtained, although this comes at the cost of writing speed.

- (6) With fabrication methods that use self-assembly of molecules, high complexity, resolutions, and diversity can be achieved. Using self-assembled patterns as templates during etching processes results in a high-throughput process, making self-assembly particularly interesting for industry.

The radar plot may be used as a decision-making tool for choosing the most suitable fabrication method(s), based on

the most relevant moderators to realize the envisioned performance of a nanostructure or microstructure. For example, suppose a researcher wants to make structures with a resolution down to 100 nm. In this case, the researcher could choose between scanning beam lithography, hard or soft molding, FIBID/FEBID, and directed self-assembly. If the envisioned structure contains overhanging features and geometric diversity is required, self-assembly methods and FIBID/FEBID are preferred. On the other hand, if relatively large structures are required at a high throughput, hard molding may be the method of preference.

Table 5 provides a comparative overview of the identified ten groups of nanofabrication and microfabrication methods in terms of the aforementioned seven moderators.

5.2. Attainable Geometric Complexity Versus Processing Characteristics

By categorizing fabrication methods based on a structure-related moderator (e.g., geometric complexity as we did in this review), fabrication methods can be assessed independently from processing characteristics such as being of additive or subtractive nature, parallel or serial (i.e., based on single-step and multistep manufacturing, respectively), etc. However, identifying the relationship between processing characteristics and the structural characteristics of the envisioned structures can provide useful insights regarding the evolution of existing fabrication methods as well as the emergence of new fabrication methods. Accordingly, in **Table 6**, we relate geometric complexity and processing characteristics for the reviewed methods. It can be seen that for level-1 geometric complexity in nanostructures or microstructures (e.g., extruded 2D structures), both additive and subtractive fabrication methods, and both serial and parallel methods, can be used, whereas structures of the highest level of complexity can only be fabricated with serial, additive methods. This also means that high geometric complexity currently can only be achieved at low throughputs. Besides, for additive, serial methods, a higher resolution is only possible with even lower writing speeds, meaning that the attainable resolution depends on the geometric complexity of a structure. Similar associations can be made between processing characteristics and other structure-related moderators.

5.3. Additive Manufacturing

One could not avoid noticing that AM (commonly referred to as 3D printing) occupies a relatively small part of our review, which may not seem in hand with the attention that this group of techniques is gaining both in academia and in industry. The reason why we did not present a more extensive overview of AM methods is that, except for vat photopolymerization methods, EHD, and LIFT, AM methods are not yet suitable

for fabricating nanostructures or microstructures. Specifically, most AM methods are solid-based, ink-based, and powder-based and use deposition mechanisms such as sintering, melting, and gluing.^[211,212] For these deposition mechanisms, a high pixel volume is required and thus true micrometer-sized features are currently not possible. Increasing the attainable resolution of such AM methods would directly add to the number of nanofabrication and microfabrication methods that can achieve microstructures with high geometric complexity.

5.4. Increasing Geometric Complexity by Postprocessing

When determining the attainable complexity of fabrication methods, we did not take into consideration postprocessing steps. It is, however, common to use fabrication methods as part of a toolbox set, together with operations such as postprocess melting, grinding, and stacking of 2D layers to obtain a 3D structure. As an example of postprocessing resulting in increased geometric complexity, del Campo et al.^[213] fabricated pillar arrays with lithographic methods, after which overhanging parts were incorporated by pressing the pillars against a surface. Alternatively, geometric complexity can be increased by doing multiple cycles of one fabrication method, to create multilayered structures. For example, Varghese et al.^[214] fabricated woodpile-like structures by means of EBL by writing in added layers on top of fabricated patterns.

5.5. Future Directions

In this review an inductive pathway of designing nanostructures and microstructures is supported by focusing on making the step from the geometric and material properties of an envisioned structure toward a fabrication method suitable for fabricating this structure (see Figure 1). To further support an inductive design pathway, the step from the desired performance toward the required geometric and material properties should be also better understood. To achieve that, a comprehensive assessment of the (attainable) performance of functional nanostructures and microstructures is needed. Here, the seven

Table 6. Fabrication methods categorized based on the geometric complexity, that can be achieved with them, versus their processing characteristics (additive or subtractive and parallel or serial).

Processing characteristics		Geometric complexity		
		Level 1	Level 2	Level 3
Additive	Serial	Laser-induced forward transfer (LIFT)		Vat photopolymerization
		Electrohydrodynamic jet printing (EHD)		Focus ion/electron beam-induced deposition (FIBID/FEBID)
	Parallel		Directed self-assembly (DSA)	
Subtractive/Additive	Serial	Scanning beam lithography (SBL)		
		Scanning probe lithography (SPL)		
Subtractive	Parallel	Photolithography	Hard molding	
			Soft molding	

identified performance-determining moderators were used in a qualitative/conceptual fashion to organize fabrication methods based on the attainable nanostructures and microstructures. Studying the quantitative effect of these, and possibly other, moderators on the performance of nanostructures and microstructures would provide useful insights into how performance can be improved.

In order to assess which characteristics of a fabrication method have the potential to improve in the future, it is important to first consider the intrinsic limitations of each method. For example, the low geometric diversity of hard and soft molding is an intrinsic limitation of these methods, as with one mold, only one structure with defined size and shape can be fabricated. As another example, the low throughput of SPL is caused by the fact that a probe can only modify single nanoscale objects or molecules. Accelerating the SPL process would be only possible at the expense of a lower resolution (an exception is thermal SPL, in which high writing speeds, up to 20 mm s⁻¹ at 15 nm resolution,^[215] can be obtained, making thermal SPL comparable with electron beam lithography in terms of throughput).

When it comes to processing characteristics of fabrication methods, next to intrinsic limitations, it is also important to note that the characteristics of a fabrication method may be interdependent. For example, the resolution of photolithography can be improved by using shorter wavelength light, combined with more precise, expensive optics. In other words, increased resolution in photolithography is possible, but for increased costs.^[87] In the future, it is likely that the resolution of vat photopolymerization methods will increase by reducing the laser focal point size.^[200] A resolution increase will come at the expense of throughput, however, since more writing steps will be required to pattern a certain area or volume. A similar trade-off between feature size and throughput applies to serial deposition methods, namely EHD and LIFT. Engstrom et al.^[19] noted that with EHD, thinner lines can be written faster than thicker lines, because the required amount of ink is lower for smaller features, given a fixed ink flow rate. While this is true for single objects like lines or pillars, throughput will decrease for smaller feature sizes, considering that smaller features also result in a higher number of features per area.

From the radar plot we can deduce that molecular-scale methods such as DSA and SPL can be improved when it comes to throughput and total size, without going at the expense of resolution or complexity. The fundamental resolution limit of more conventional nanofabrication methods (such as photolithography) is still an order of magnitude above the molecular-scale resolutions that DSA and SPL attain, showing their promise for nanofabrication.

5.6. Conclusion

In this paper, we reviewed nanofabrication and microfabrication methods based on the geometric complexity that they can achieve, independently from processing characteristics, and with material complexity, resolution, total size of the structure, geometric diversity, material diversity, and throughput as moderators. A geometric complexity-based categorization

of nanofabrication and microfabrication methods facilitates the decision-making for identifying the most suitable method for fabricating functional nanostructures or microstructures with predefined properties. Furthermore, such a categorization provides a framework for systematically organizing fabrication methods across application fields. This allows designers of nanostructures and microstructures to include a wide range of fabrication methods in their design considerations.

Acknowledgements

This research was supported by the Netherlands Organization for Scientific Research (NWO) Domain Applied and Engineering Sciences (TTW) (Open Technology Program, project 13353 “Secure and gentle grip of delicate biological tissues”).

Conflict of Interest

The authors declare no conflict of interest.

Keywords

microfabrication, microstructures, nanofabrication, nanostructures

Received: September 29, 2017

Revised: November 30, 2017

Published online: March 24, 2018

- [1] G. E. Moore, *IEEE Solid-State Circuits Soc. Newsl.* **2006**, *11*, 37.
- [2] G. E. Moore, *Proc. IEEE* **1998**, *86*, 82.
- [3] S. Nishimoto, B. Bhushan, *RSC Adv.* **2013**, *3*, 671.
- [4] D. M. Drotlef, L. Stepien, M. Kappl, W. J. P. Barnes, H. J. Butt, A. del Campo, *Adv. Funct. Mater.* **2013**, *23*, 1137.
- [5] H. Lee, B. P. Lee, P. B. Messersmith, *Nature* **2007**, *448*, 338.
- [6] J. Iturri, L. Xue, M. Kappl, L. García-Fernández, W. J. P. Barnes, H.-J. Butt, A. del Campo, *Adv. Funct. Mater.* **2015**, *25*, 1499.
- [7] W. L. Min, B. Jiang, P. Jiang, *Adv. Mater.* **2008**, *20*, 3914.
- [8] C. Lucarotti, C. M. Oddo, N. Vitiello, M. C. Carrozza, *Sensors* **2013**, *13*, 1435.
- [9] F. de Gaetano, P. Bagnoli, A. Zaffora, A. Pandolfi, M. Serrani, J. Brubert, J. Stasiak, G. D. Moggridge, M. L. Costantino, *J. Mech. Med. Biol.* **2015**, *15*, 1540009.
- [10] S. L. Lin, C. C. Lin, D. Y. Lin, C. S. Chuang, in *8th Annu. IEEE Int. Conf. Nano/Micro Eng. Mol. Syst.*, IEEE, Piscataway, NJ, USA **2013**, pp. 594–597.
- [11] M. López-Álvarez, C. Rodríguez-Valencia, J. Serra, P. González, *Procedia Eng.* **2013**, *59*, 51.
- [12] J. F. Swennenhuis, A. G. J. Tibbe, M. Stevens, M. R. Katika, J. van Dalum, H. Duy Tong, C. J. M. van Rijn, L. W. M. M. Terstappen, *Lab Chip* **2015**, *15*, 3039.
- [13] J. Swennenhuis, A. G. J. Tibbe, C. J. M. van Rijn, L. W. M. M. Terstappen, *Lab Chip* **2015**, *15*, 3039.
- [14] E. K. Sackmann, A. L. Fulton, D. J. Beebe, *Nature* **2014**, *507*, 181.
- [15] P. J. Kitson, M. H. Rosnes, V. Sans, V. Dragone, L. Cronin, *Lab Chip* **2012**, *12*, 3267.

- [16] D. Rochette, B. Kent, A. Habicht, S. Seiffert, *Colloid Polym. Sci.* **2017**, 295, 507.
- [17] M. M. Hamed, B. Ünal, E. Kerr, A. C. Glavan, M. T. Fernandez-Abedul, G. M. Whitesides, *Lab Chip* **2016**, 16, 3885.
- [18] M. M. Waldrop, *Nature* **2016**, 530, 144.
- [19] D. S. Engstrom, B. Porter, M. Pacios, H. Bhaskaran, *J. Mater. Res.* **2014**, 29, 1792.
- [20] M. Röhrig, M. Thiel, M. Worgull, H. Hölscher, *Small* **2012**, 8, 3009.
- [21] X. Li, Y. Cao, M. Gu, *Opt. Lett.* **2011**, 36, 2510.
- [22] Z. Doubrovski, J. C. Verlinden, J. M. P. Geraedts, *ASME Int. Des. Eng. Tech. Conf. Comput. Inf. Eng. Conf., Proc.* **2011**, 9, 635.
- [23] B. D. Gates, Q. Xu, M. Stewart, D. Ryan, C. G. Willson, G. M. Whitesides, *Chem. Rev.* **2005**, 105, 1171.
- [24] M. C. Traub, W. Longsine, V. N. Truskett, *Annu. Rev. Chem. Biomol. Eng.* **2016**, 7, 583.
- [25] S. Y. Chou, P. R. Krauss, W. Zhang, L. Guo, L. Zhuang, *J. Vac. Sci. Technol., B: Microelectron. Nanometer Struct.–Process., Meas., Phenom.* **1997**, 15, 2897.
- [26] M. N. Costa, B. Veigas, J. M. Jacob, D. S. Santos, J. Gomes, P. V. Baptista, R. Martins, J. Inácio, E. Fortunato, *Nanotechnology* **2014**, 25, 094006.
- [27] E. Brinksmeier, O. Riemer, R. Stern, in *Initiatives of Precision Engineering at the Beginning of a Millennium* (Ed.: I. Inasaki), Kluwer Academic Publishers, Boston, USA **2001**, pp. 3–11.
- [28] Y. Qin, A. Brockett, Y. Ma, A. Razali, J. Zhao, C. Harrison, W. Pan, X. Dai, D. Loziak, *Int. J. Adv. Des. Manuf. Technol.* **2010**, 47, 821.
- [29] A. R. Razali, Y. Qin, *Procedia Eng.* **2013**, 53, 665.
- [30] S. S. Dimov, C. W. Matthews, A. Glanfield, P. Dorrington, in *4M 2006 – Second Int. Conf. Multi-Material Micro Manuf.*, Elsevier, Amsterdam, the Netherlands **2006**, pp. xi–xxv.
- [31] M. Vaezi, H. Seitz, S. Yang, *Int. J. Adv. Des. Manuf. Technol.* **2013**, 67, 1721.
- [32] G. B. Olson, *Science* **1997**, 277, 1237.
- [33] D. L. D. Bourell, J. J. Beaman, M. C. Leu, D. W. Rosen, in *US-Turkey workshop on rapid technologies*, Wohlers Associates, Fort Collins, Colorado, USA **2009**, p. 5.
- [34] Z. Gan, Y. Cao, R. A. Evans, M. Gu, *Nat. Commun.* **2013**, 4, 2061.
- [35] L. Heepe, S. N. Gorb, *Annu. Rev. Mater. Res.* **2014**, 41, 110301100446097.
- [36] D. Brodoceanu, C. T. Bauer, E. Kroner, E. Arzt, T. Kraus, *Bioinspiration Biomimetics* **2016**, 11, 051001.
- [37] C. Greiner, A. del Campo, E. Arzt, *Langmuir* **2007**, 23, 3495.
- [38] L. Xue, B. Sanz, A. Luo, K. T. Turner, X. Wang, D. Tan, R. Zhang, H. Du, M. Steinhart, C. Mijangos, M. Guttman, M. Kappl, A. del Campo, *ACS Nano* **2017**, 11, 9711.
- [39] A. Ghosh, B. Corves, *Introduction to Micromechanisms and Microactuators*, Vol. 28, Springer, New York, NY, USA **2015**, p. 35.
- [40] M. Li, H. X. Tang, M. L. Roukes, *Nat. Nanotechnol.* **2007**, 2, 114.
- [41] M. Esashi, S. Tanaka, *Micromachines* **2016**, 7, 137.
- [42] T. Brecht, W. Pfaff, C. Wang, Y. Chu, L. Frunzio, M. H. Devoret, R. J. Schoelkopf, *npj Quantum Information* **2016**, 2, 16002.
- [43] Q. Liu, X. Duan, C. Peng, *Novel Optical Technologies for Nanofabrication*, Springer, New York, NY, USA **2014**.
- [44] N. Khusnatdinov, Z. Ye, K. Luo, T. Stachowiak, X. Lu, J. W. Irving, M. Shafraan, W. Longsine, M. Traub, V. Truskett, B. Fletcher, W. Liu, F. Xu, D. LaBrake, S. V. Sreenivasan, *Proc. SPIE* **2014**, 9049, 904910.
- [45] S. R. J. Brueck, *Proc. IEEE* **2005**, 93, 1704.
- [46] S. Chou, *Nanoimprint Lithography*, Woodhead Publishing Limited, Sawston, UK **1996**.
- [47] Q. Yang, J. Liu, H. Li, Y. Li, J. Hou, M. Li, Y. Song, *RSC Adv.* **2015**, 5, 11096.
- [48] L. K. Grunenfelder, S. Herrera, D. Kisailus, *Small* **2014**, 10, 3207.
- [49] W. Federle, W. J. P. Barnes, W. Baumgartner, P. Drechsler, J. M. Smith, *J. R. Soc., Interface* **2006**, 3, 689.
- [50] A. Tulchinsky, A. D. Gat, *J. Fluid Mech.* **2015**, 775, 188.
- [51] A. Chworos, W. Smitthipong, in *Bio-Based Composites for High-Performance Materials*, CRC Press, Boca Raton, FL, USA **2014**, pp. 43–58.
- [52] U. G. K. Wegst, H. Bai, E. Saiz, A. P. Tomsia, R. O. Ritchie, *Nat. Mater.* **2015**, 14, 23.
- [53] R. O. Ritchie, *Nat. Mater.* **2011**, 10, 817.
- [54] L. K. Grunenfelder, N. Suksangpanya, C. Salinas, G. Milliron, N. Yaraghi, S. Herrera, K. Evans-Lutterodt, S. R. Nutt, P. Zavattieri, D. Kisailus, *Acta Biomater.* **2014**, 10, 3997.
- [55] R. Courant, H. Robbins, I. Stewart, *What Is Mathematics? An Elementary Approach to Ideas and Methods*, OUP, US **1996**.
- [56] S. Reuter, M. A. Smolarczyk, A. Istock, U. M. Ha, O. Schneider, N. Worapattarakul, S. Nazemroaya, H. Hoang, L. Gomer, F. Pilger, M. Maniak, H. Hillmer, *J. Nanopart. Res.* **2017**, 19, 184.
- [57] S. Uchida, N. Ozaki, T. Nakahama, H. Oda, N. Ikeda, Y. Sugimoto, *Jpn. J. Appl. Phys.* **2017**, 56, 050303.
- [58] C. Greiner, E. Arzt, A. del Campo, *Adv. Mater.* **2009**, 21, 479.
- [59] K. Cicha, T. Koch, J. Torgersen, Z. Li, R. Liska, J. Stampfl, *J. Appl. Phys.* **2012**, 112, 094906.
- [60] O. Tricinci, T. Terencio, B. Mazzolai, N. M. Pugno, F. Greco, V. Mattoli, *ACS Appl. Mater. Interfaces* **2015**, 7, 25560.
- [61] R. Garcia, A. W. Knoll, E. Riedo, *Nat. Nanotechnol.* **2014**, 9, 577.
- [62] A. W. Knoll, D. Pires, O. Coulembier, P. Dubois, J. L. Hedrick, J. Frommer, U. Duerig, *Adv. Mater.* **2010**, 22, 3361.
- [63] K. Brown, D. J. Eichelsdoerfer, X. Liao, S. He, C. A. Mirkin, *Front. Phys.* **2014**, 9, 385.
- [64] K. M. Carroll, X. Lu, S. Kim, Y. Gao, H.-J. Kim, S. Somnath, L. Polloni, R. Sordan, W. P. King, J. E. Curtis, *Nanoscale* **2014**, 6, 1299.
- [65] S. Hong, *Science* **1999**, 286, 523.
- [66] O. A. Nafday, J. R. Haaheim, F. Villagran, *Scanning* **2009**, 31, 122.
- [67] K. Salaita, Y. Wang, C. A. Mirkin, *Nat. Nanotechnol.* **2007**, 2, 145.
- [68] Y. Wang, D. Maspoch, S. Zou, G. C. Schatz, R. E. Smalley, C. A. Mirkin, *Proc. Natl. Acad. Sci. USA* **2006**, 103, 2026.
- [69] L. Chen, X. Wei, X. Zhou, Z. Xie, K. Li, Q. Ruan, C. Chen, J. Wang, C. A. Mirkin, Z. Zheng, *Small* **2017**, 13, 1702003.
- [70] R. Ferris, A. Hucknall, B. S. Kwon, T. Chen, A. Chilkoti, S. Zauscher, *Small* **2011**, 7, 3032.
- [71] F. Holzner, P. Paul, M. Despont, L. L. Cheong, J. Hedrick, U. Dürig, A. Knoll, *Proc. SPIE* **2013**, 8886, 888605.
- [72] Y. K. Ryu Cho, C. D. Rawlings, H. Wolf, M. Spieser, S. Bisig, S. Reidt, M. Sousa, S. R. Khanal, T. D. B. Jacobs, A. W. Knoll, *ACS Nano* **2017**, 11, 11890.
- [73] J. A. Dagata, J. Schneir, H. H. Harary, C. J. Evans, M. T. Postek, J. Bennett, *Appl. Phys. Lett.* **1990**, 56, 2001.
- [74] A. A. O. Elkaseh, W. J. Perold, V. V. Srinivasu, *J. Appl. Phys.* **2010**, 108, 053914.
- [75] J. Zhao, L. A. Swartz, W. Lin, P. S. Schlenoff, J. Frommer, J. B. Schlenoff, G. Liu, *ACS Nano* **2016**, 10, 5656.
- [76] H. Ito, *Adv. Polym. Sci.* **2005**, 172, 37.
- [77] B. J. Kim, E. Meng, *J. Microelectr. Microeng.* **2016**, 26, 013001.
- [78] S. Okazaki, *Microelectron. Eng.* **2015**, 133, 23.
- [79] P. Clarke, Intel Orders 15 EUV Lithography Systems, **2015**.
- [80] TWINSKAN NXE : 3400B. *Technical Specifications*, **2017**.
- [81] A. R. Abate, P. Mary, V. van Steijn, D. A. Weitz, *Lab Chip* **2012**, 12, 1516.
- [82] P. Zhu, L. Wang, *Lab Chip* **2017**, 17, 34.
- [83] A. Pimpin, W. Srituravanich, *Eng. J.* **2012**, 16, 37.
- [84] N. Mojarad, J. Gobrecht, Y. Ekinici, *Microelectron. Eng.* **2015**, 143, 55.
- [85] J. Fischer, M. Wegener, *Laser Photonics Rev.* **2013**, 7, 22.

- [86] E. Buitrago, R. Fallica, D. Fan, T. S. Kulmala, M. Vockenhuber, Y. Ekinci, *Microelectron. Eng.* **2016**, 155, 44.
- [87] C. Wagner, N. Harned, *Nat. Photonics* **2010**, 4, 24.
- [88] N. Mojarad, M. Hojeij, L. Wang, J. Gobrecht, Y. Ekinci, *Nanoscale* **2015**, 7, 4031.
- [89] J. Melngailis, *J. Vac. Sci. Technol., B: Microelectron. Nanometer Struct.–Process., Meas., Phenom.* **1998**, 16, 927.
- [90] F. Watt, A. A. Bettiol, J. A. van Kan, E. J. Teo, M. B. H. Breese, *Int. J. Nanosci.* **2005**, 4, 269.
- [91] S. Danylyuk, H. Kim, S. Brose, C. Dittberner, P. Loosen, T. Taubner, K. Bergmann, L. Juschkina, *J. Vac. Sci. Technol., B: Nanotechnol. Microelectron.: Mater., Process., Meas., Phenom.* **2013**, 31, 21602.
- [92] G. Kunkemöller, T. W. W. Maß, A.-K. U. Michel, H.-S. Kim, S. Brose, S. Danylyuk, T. Taubner, L. Juschkina, *Opt. Express* **2015**, 23, 25487.
- [93] L. Markey, F. Zacharatos, J.-C. Weeber, A. Prinzen, M. Waldow, M. G. Nielsen, T. Tekin, A. Dereux, *Microelectron. Eng.* **2015**, 141, 129.
- [94] Y. Chen, J. Qin, J. Chen, L. Zhang, C. Ma, J. Chu, X. Xu, L. Wang, *Nanotechnology* **2017**, 28, 055302.
- [95] A. Doolittle, *Lithography and Pattern Transfer*, **2008**.
- [96] J. Dong, J. Liu, G. Kang, J. Xie, Y. Wang, *Sci. Rep.* **2015**, 4, 5618.
- [97] L. Pan, Y. Park, Y. Xiong, E. Ulin-Avila, Y. Wang, L. Zeng, S. Xiong, J. Rho, C. Sun, D. B. Bogy, X. Zhang, *Sci. Rep.* **2011**, 1, 1.
- [98] L. Bruchhaus, S. Bauderick, L. Peto, U. Barth, A. Rudzinski, J. Mussmann, J. Klingfus, J. Gierak, H. Hövel, *Microelectron. Eng.* **2012**, 97, 48.
- [99] Z. Gan, Y. Cao, R. A. Evans, M. Gu, *Nat. Commun.* **2013**, 4, 2061.
- [100] J.-H. Jang, C. K. Ullal, M. Maldovan, T. Gorishnyy, S. Kooi, C. Koh, E. L. Thomas, *Adv. Funct. Mater.* **2007**, 17, 3027.
- [101] B. Päiväranta, A. Langner, E. Kirk, C. David, Y. Ekinci, *Nanotechnology* **2011**, 22, 375302.
- [102] A. A. Tseng, K. Chen, C. D. Chen, K. J. Ma, *IEEE Trans. Electron. Packag. Manuf.* **2003**, 26, 141.
- [103] N. Arjmandi, L. Lagae, G. Borghs, *J. Vac. Sci. Technol., B: Microelectron. Nanometer Struct.–Process., Meas., Phenom.* **2009**, 27, 1915.
- [104] V. R. Manfrinato, L. Zhang, D. Su, H. Duan, R. G. Hobbs, E. A. Stach, K. K. Berggren, *Nano Lett.* **2013**, 13, 1555.
- [105] A. Joshi-Imre, S. Bauderick, *J. Nanotechnol.* **2014**, 2014, 1.
- [106] R. L. Kubena, *J. Vac. Sci. Technol., B: Microelectron. Nanometer Struct.–Process., Meas., Phenom.* **1991**, 9, 3079.
- [107] J. Gierak, A. Septier, C. Vieu, *Nucl. Instrum. Methods Phys. Res., Sect. A* **1999**, 427, 91.
- [108] C. M. Bates, M. J. Maher, D. W. Janes, C. J. Ellison, C. G. Willson, *Macromolecules* **2014**, 47, 2.
- [109] S. Ji, L. Wan, C. C. Liu, P. F. Nealey, *Prog. Polym. Sci.* **2016**, 54–55, 76.
- [110] S. B. Darling, *Prog. Polym. Sci.* **2007**, 32, 1152.
- [111] S. M. Douglas, H. Dietz, T. Liedl, B. Hogberg, F. Graf, W. M. Shih, *Nature* **2009**, 459, 414.
- [112] V. K. Khanna, *Integrated Nanoelectronics Nanoscale CMOS, Post-CMOS and Allied Nanotechnologies*, Springer, India **2016**.
- [113] Y. C. Tseng, Q. Peng, L. E. Ocola, J. W. Elam, S. B. Darling, *J. Phys. Chem. C* **2011**, 115, 17725.
- [114] C. J. Hawker, T. P. Russell, *MRS Bull.* **2005**, 30, 952.
- [115] C.-C. Chang, D. Botez, Lei Wan, P. F. Nealey, S. Ruder, T. F. Kuech, *J. Vac. Sci. Technol., B: Nanotechnol. Microelectron.: Mater., Process., Meas., Phenom.* **2013**, 31, 031801.
- [116] M. S. Onses, C. Song, L. Williamson, E. Sutanto, P. M. Ferreira, A. G. Alleyne, P. F. Nealey, H. Ahn, J. A. Rogers, *Nat. Nanotechnol.* **2013**, 8, 667.
- [117] J. W. Jeong, W. I. Park, M. J. Kim, C. A. Ross, Y. S. Jung, *Nano Lett.* **2011**, 11, 4095.
- [118] B. H. Kim, J. Y. Kim, S. O. Kim, *Soft Matter* **2013**, 9, 2780.
- [119] M. P. Stoykovich, H. Kang, K. C. Daoulas, G. Liu, C. C. Liu, J. J. de Pablo, M. Müller, P. F. Nealey, *ACS Nano* **2007**, 1, 168.
- [120] M. Stefik, S. Guldin, S. Vignolini, U. Wiesner, U. Steiner, *Chem. Soc. Rev.* **2015**, 44, 5076.
- [121] K. Askar, B. M. Phillips, Y. Fang, B. Choi, N. Gozubenli, P. Jiang, B. Jiang, *Colloids Surf., A* **2013**, 439, 84.
- [122] H. J. Nam, J. H. Kim, D. Y. Jung, J. B. Park, H. S. Lee, *Appl. Surf. Sci.* **2008**, 254, 5134.
- [123] J. Zhang, Y. Li, X. Zhang, B. Yang, *Adv. Mater.* **2010**, 22, 4249.
- [124] K. A. Willets, R. P. van Duyne, *Annu. Rev. Phys. Chem.* **2007**, 58, 267.
- [125] J. Zhang, B. Yang, *Adv. Funct. Mater.* **2010**, 20, 3411.
- [126] S. Akerboom, J. Appel, D. Labonte, W. Federle, J. Sprakel, M. Kamperman, *J. R. Soc., Interface* **2014**, 12, 20141061.
- [127] H. M. Powell, J. J. Lannutti, *Langmuir* **2003**, 19, 9071.
- [128] D. G. Choi, H. K. Yu, S. G. Jang, S. M. Yang, *J. Am. Chem. Soc.* **2004**, 126, 7019.
- [129] C. Cong, W. Junus, Z. Shen, T. Yu, *Nanoscale Res. Lett.* **2009**, 4, 1324.
- [130] G. Zhang, D. Wang, H. Möhwald, *Nano Lett.* **2005**, 5, 143.
- [131] H. H. Masuda, K. Fukuda, P. M. Chaikin, *Science* **1995**, 268, 1466.
- [132] A. Belwalkar, E. Grasing, W. van Geertruyden, Z. Huang, W. Z. Misiolek, *J. Membr. Sci.* **2008**, 319, 192.
- [133] W. J. Stępniewski, D. Forbot, M. Norek, M. Michalska-Domańska, A. Król, *Electrochim. Acta* **2014**, 133, 57.
- [134] J. G. Buijnsters, R. Zhong, N. Tsyntsar, J.-P. Celis, *ACS Appl. Mater. Interfaces* **2013**, 5, 3224.
- [135] A. Y. Y. Ho, L. P. Yeo, Y. C. Lam, I. Rodríguez, *ACS Nano* **2011**, 5, 1897.
- [136] N. Vogel, L. de Viguerie, U. Jonas, C. K. Weiss, K. Landfester, *Adv. Funct. Mater.* **2011**, 21, 3064.
- [137] S. J. Jeong, J. Y. Kim, B. H. Kim, H. S. Moon, S. O. Kim, *Mater. Today* **2013**, 16, 468.
- [138] L. Hirt, A. Reiser, R. Spolenak, T. Zambelli, *Adv. Mater.* **2017**, 29, 1604211.
- [139] M. Yu, K. H. Ahn, S. J. Lee, *Mater. Des.* **2016**, 89, 109.
- [140] J.-U. Park, M. Hardy, S. J. Kang, K. Barton, K. Adair, D. K. Mukhopadhyay, C. Y. Lee, M. S. Strano, A. G. Alleyne, J. G. Georgiadis, P. M. Ferreira, J. A. Rogers, *Nat. Mater.* **2007**, 6, 782.
- [141] E. Sutanto, K. Shigeta, Y. K. Kim, P. G. Graf, D. J. Hoelzle, K. L. Barton, A. G. Alleyne, P. M. Ferreira, J. A. Rogers, *J. Micromech. Microeng.* **2012**, 22, 045008.
- [142] C. W. Visser, R. Pohl, C. Sun, G. W. Römer, B. Huis in 't Veld, D. Lohse, *Adv. Mater.* **2015**, 27, 4087.
- [143] M. Zenou, Z. Kotler, *Opt. Express* **2016**, 24, 1431.
- [144] B. W. An, K. Kim, H. Lee, S. Y. Kim, Y. Shim, D. Y. Lee, J. Y. Song, J. U. Park, *Adv. Mater.* **2015**, 27, 4322.
- [145] L. Peng, Y. Deng, P. Yi, X. Lai, *J. Micromech. Microeng.* **2014**, 24, 013001.
- [146] L. J. Guo, *Adv. Mater.* **2007**, 19, 495.
- [147] Q. Xia, R. F. Pease, *Nanotechnology* **2015**, 26, 182501.
- [148] H. Schiff, *Appl. Phys. A* **2015**, 121, 415.
- [149] M. D. Stewart, S. C. Johnson, S. V. Sreenivasan, D. J. Resnick, C. G. Willson, *J. Microlithogr. Microfabr., Microsyst.* **2005**, 4, 011002.
- [150] S. Y. Chou, P. R. Krauss, P. J. Renstrom, *Appl. Phys. Lett.* **1995**, 67, 3114.
- [151] S. H. Ahn, L. J. Guo, *Adv. Mater.* **2008**, 20, 2044.
- [152] G. Calafiore, A. Koshelev, F. I. Allen, S. Dhuey, S. Sassolini, E. Wong, P. Lum, K. Munechika, S. Cabrini, *Nanotechnology* **2016**, 27, 375301.
- [153] H. Küpers, A. Tahraoui, R. B. Lewis, S. Rauwerdink, M. Matalla, O. Krüger, F. Bastiman, H. Riechert, L. Geelhaar, *Semicond. Sci. Technol.* **2017**, 32, 115003.
- [154] I. Fernandez-Cuesta, A. Laura Palmarelli, X. Liang, J. Zhang, S. Dhuey, D. Olynick, S. Cabrini, *J. Vac. Sci. Technol.*

- B: Nanotechnol. Microelectron.: Mater., Process., Meas., Phenom.* **2011**, 29, 06F801.
- [155] K. Ansari, J. A. van Kan, A. A. Bettiol, F. Watt, *Appl. Phys. Lett.* **2004**, 85, 476.
- [156] D. J. Resnick, W. J. Dauksher, D. Mancini, K. J. Nordquist, E. Ainley, K. Gehoski, J. H. Baker, T. C. Bailey, B. J. Choi, S. Johnson, S. V. Sreenivasan, J. G. Ekerdt, C. G. Willson, *J. Microlithogr., Microfabr., Microsyst.* **2002**, 1, 284.
- [157] M. Nakagawa, A. Nakaya, Y. Hoshikawa, S. Ito, N. Hiroshiba, T. Kyotani, *ACS Appl. Mater. Interfaces* **2016**, 8, 30628.
- [158] D. Jucius, A. Lazauskas, V. Grigaliūnas, B. Abakevičienė, S. Smetona, S. Tamulevičius, *Microsyst. Technol.* **2018**, 24, 1115.
- [159] M. D. Stewart, S. C. Johnson, S. V. Sreenivasan, D. J. Resnick, C. G. Willson, *J. Microlithogr., Microfabr., Microsyst.* **2005**, 4, 11002.
- [160] W.-D. Li, W. Wu, R. Stanley Williams, *J. Vac. Sci. Technol., B: Nanotechnol. Microelectron.: Mater., Process., Meas., Phenom.* **2012**, 30, 06F304.
- [161] Y. Xia, J. J. McClelland, R. Gupta, D. Qin, X. M. Zhao, L. L. Sohn, R. J. Celotta, G. M. Whitesides, *Adv. Mater.* **1997**, 9, 147.
- [162] E. King, Y. Xia, X. M. Zhao, G. M. Whitesides, *Adv. Mater.* **1997**, 9, 651.
- [163] Y. Xia, G. M. Whitesides, *Annu. Rev. Mater. Sci.* **1998**, 28, 153.
- [164] N. L. Jeon, R. G. Nuzzo, Y. Xia, M. Mrksich, G. M. Whitesides, *Langmuir* **1995**, 11, 3024.
- [165] M. Heckele, W. K. Schomburg, *J. Micromech. Microeng.* **2004**, 14, R1.
- [166] C. N. LaFratta, T. Baldacchini, R. A. Farrer, J. T. Fourkas, M. C. Teich, B. E. A. Saleh, M. J. Naughton, *J. Phys. Chem. B* **2004**, 108, 11256.
- [167] H.-H. Jeong, J.-H. Lee, Y.-M. Noh, Y.-G. Kim, C.-S. Lee, *Macromol. Res.* **2013**, 21, 534.
- [168] D. Pisignano, E. Sariconi, M. Mazzeo, G. Gigli, R. Cingolani, *Adv. Mater.* **2002**, 14, 1565.
- [169] L. Han, J. Zhou, X. Gong, C. Gao, *Chin. Sci. Bull.* **2009**, 54, 2193.
- [170] D. Liyu, S. H. Nemati, A. E. Vasdekis, *J. Polym. Sci., Part B: Polym. Phys.* **2016**, 54, 1681.
- [171] E. Müller, T. Pompe, U. Freudenberg, C. Werner, *Adv. Mater.* **2017**, 29, 1703489.
- [172] F. Hua, Y. Sun, A. Gaur, M. A. Meitl, L. Bilhaut, L. Rotkina, J. Wang, P. Geil, M. Shim, J. A. Rogers, A. Shim, *Nano Lett.* **2004**, 4, 2467.
- [173] Z. X. Deng, C. D. Mao, *Langmuir* **2004**, 20, 8078.
- [174] C. Pang, T. Kim, W. G. Bae, D. Kang, S. M. Kim, K.-Y. Suh, *Adv. Mater.* **2012**, 24, 475.
- [175] J. A. Helmuth, H. Schmid, R. Stutz, A. Stemmer, H. Wolf, *J. Am. Chem. Soc.* **2006**, 128, 9296.
- [176] J. C. Love, L. A. Estroff, J. K. Kriebel, R. G. Nuzzo, G. M. Whitesides, *Chem. Rev.* **2005**, 105, 1103.
- [177] S. Alom Ruiz, C. S. Chen, *Soft Matter* **2007**, 3, 168.
- [178] S. A. Lange, V. Benes, D. P. Kern, J. K. H. Ho, *Anal. Chem.* **2004**, 76, 1641.
- [179] S. T. Han, Y. Zhou, Z. X. Xu, L. B. Huang, X. B. Yang, V. A. L. Roy, *Adv. Mater.* **2012**, 24, 3556.
- [180] Y. Xia, G. M. Whitesides, *Langmuir* **1997**, 13, 2059.
- [181] M. K. Choi, J. Yang, K. Kang, D. C. Kim, C. Choi, C. Park, S. J. Kim, S. I. Chae, T.-H. Kim, J. H. Kim, T. Hyeon, D.-H. Kim, *Nat. Commun.* **2015**, 6, 7149.
- [182] J. Li, L. Xu, S. Kim, A. A. Shestopalov, *J. Mater. Chem. C* **2016**, 4, 4155.
- [183] J. W. Jeong, S. R. Yang, Y. H. Hur, S. W. Kim, K. M. Baek, S. Yim, H.-I. Jang, J. H. Park, S. Y. Lee, C.-O. Park, Y. S. Jung, *Nat. Commun.* **2014**, 5, 5387.
- [184] J.-G. Kim, Y. Sim, Y. Cho, J.-W. Seo, S. Kwon, J.-W. Park, H. G. Choi, H. Kim, S. Lee, *Microelectron. Eng.* **2009**, 86, 2427.
- [185] D. J. Resnick, S. V. Sreenivasan, C. G. Willson, *Mater. Today* **2005**, 8, 34.
- [186] M. B. Chan-Park, J. Zhang, Y. Yan, C. Y. Yue, *Sens. Actuators B* **2004**, 101, 175.
- [187] R. Gauvin, Y. C. Chen, J. W. Lee, P. Soman, P. Zorlutuna, J. W. Nichol, H. Bae, S. Chen, A. Khademhosseini, *Biomaterials* **2012**, 33, 3824.
- [188] C. Maurer, A. Jesacher, S. Bernet, M. Ritsch-Marte, *Laser Photon. Rev.* **2011**, 5, 81.
- [189] J. K. Hohmann, M. Renner, E. H. Waller, G. von Freymann, *Adv. Opt. Mater.* **2015**, 3, 1488.
- [190] G. Vizsnyiczai, L. Kelemen, P. Ormos, *Phys. A* **2010**, 100, 181.
- [191] C. W. Hull, S. T. Spence, D. J. Albert, D. R. Smalley, R. A. Harlow, P. Stinebaugh, H. L. Tarnoff, H. D. Nguyen, C. W. Lewis, T. J. Vorigitch, D. Z. Remba, *U.S. Patent No 5*, **1993**, 184, 307.
- [192] Q. Chen, R. Xu, Z. He, K. Zhao, L. Pan, *J. Electrochem. Soc.* **2017**, 164, A1852.
- [193] A. A. Yazdi, A. Popma, W. Wong, T. Nguyen, Y. Pan, J. Xu, *Microfluid. Nanofluid.* **2016**, 20, 1.
- [194] M. Malinauskas, M. Farsari, A. Piskarskas, S. Juodkazis, *Phys. Rep.* **2013**, 533, 1.
- [195] E. S. Wu, J. H. Strickler, W. R. Harrell, W. W. Webb, *Proc. SPIE* **1992**, 1674, 776.
- [196] P. Mueller, M. Thiel, M. Wegener, *Opt. Lett.* **2014**, 39, 6847.
- [197] J. Fischer, M. Wegener, *Opt. Mater. Express* **2011**, 1, 2363.
- [198] P. E. Petrochenko, J. Torgersen, P. Gruber, L. A. Hicks, J. Zheng, G. Kumar, R. J. Narayan, P. L. Goering, R. Liska, J. Stampfl, A. Ovsianikov, *Adv. Healthcare Mater.* **2015**, 4, 739.
- [199] R. Gupta, J. Fréchet, *Langmuir* **2012**, 28, 14703.
- [200] K. S. Lee, D.-Y. Yang, S. H. Park, T. W. Lim, R. H. Kim, in *2006 Int. Symp. Biophotonics, Nanophotonics Metamaterials*, IEEE, Piscataway, NJ, USA **2006**, p. 8–14.
- [201] A. Fernández-Pacheco, L. Serrano-Ramón, J. M. Michalik, M. R. Ibarra, J. M. de Teresa, L. O'Brien, D. Petit, J. Lee, R. P. Cowburn, *Sci. Rep.* **2013**, 3, 1492.
- [202] W. F. van Dorp, C. W. Hagen, *J. Appl. Phys.* **2008**, 104, 081301.
- [203] M. Esposito, V. Tasco, F. Todisco, A. Benedetti, D. Sanvitto, A. Passaseo, *Adv. Opt. Mater.* **2014**, 2, 154.
- [204] A. J. M. Mackus, N. F. W. Thissen, J. J. L. Mulders, P. H. F. Trompenaars, Z. Chen, W. M. M. Kessels, A. A. Bol, *Appl. Phys. Lett.* **2017**, 110, 013101.
- [205] H. Cölfen, S. Mann, *Angew. Chem., Int. Ed.* **2003**, 42, 2350.
- [206] R. Gramage-Doria, J. Hessels, S. H. A. M. Leenders, O. Tröppner, M. Dürr, I. Ivanović-Burmazovi, J. N. H. Reek, *Angew. Chem., Int. Ed.* **2014**, 53, 13380.
- [207] S. Mura, J. Nicolas, P. Couvreur, *Nat. Mater.* **2013**, 12, 991.
- [208] M. Ulbricht, *Polymer* **2006**, 47, 2217.
- [209] M. A. Cohen Stuart, W. T. S. Huck, J. Genzer, M. Müller, C. Ober, M. Stamm, G. B. Sukhorukov, I. Szleifer, V. V. Tsukruk, M. Urban, F. Winnik, S. Zauscher, I. Luzinov, S. Minko, *Nat. Mater.* **2010**, 9, 101.
- [210] S. Akerboom, S. P. Pujari, A. Turak, M. Kamperman, *ACS Appl. Mater. Interfaces* **2015**, 7, 16507.
- [211] K. V. Wong, A. Hernandez, *ISRN Mech. Eng.* **2012**, 2012, 1.
- [212] N. Guo, M. C. Leu, *Front. Mech. Eng.* **2013**, 8, 215.
- [213] A. del Campo, C. Greiner, E. Arzt, *Langmuir* **2007**, 23, 10235.
- [214] L. T. Varghese, L. Fan, J. Wang, Y. Xuan, M. Qi, *Small* **2013**, 9, 4237.
- [215] A. W. Knoll, M. Zientek, L. L. Cheong, C. Rawlings, P. Paul, F. Holzner, J. L. Hedrick, D. J. Coady, R. Allen, U. Dürig, *SPIE Adv. Lithogr.* **2014**, 11, 90490B.